

GRAVITY GRADIOMETER DATA REDUCTION

Thesis by

Robert James Glaser

In Partial Fulfillment of the Requirements

For the Degree of

Aeronautical Engineer

California Institute of Technology

Pasadena, California

1972

(Submitted September 18, 1972)

ACKNOWLEDGMENT

The author first came in contact with the gravity gradiometer through the efforts of Dr. E. J. Sherry who arranged for the author to define gravity gradiometer satellite constraints as a summer job at the Jet Propulsion Laboratory (JPL). This proved nearly impossible without some idea of what could be done to reduce the gradiometer data, a project outside the scope of the JPL study. Thus the author was lead to pursue gradiometer data reduction as a thesis topic. Dr. H. J. Stewart was kind enough to be persuaded to direct the work at Caltech. As the author's committee chairman, Dr. Stewart proved to be an interested and authoritative advisor, especially as regards the myriad equations surrounding associated Legendre polynomials.

Throughout the effort surrounding a work of this type, the author has received superb support from a large number of people both at JPL and Caltech. At JPL, Dr. Sherry and Dr. A. A. Loomis stand out in particular. Dr. Loomis, a Geologist specializing in gravity and the program's Project Scientist, played a valuable role in keeping the author from pursuing the wilder schemes the author hatched. JPL also supplied the author's computer budget, \$300. At Caltech, the author's committee: Dr. Stewart, Dr. D. E. Coles, and Dr. P. Dergarabedian proved to be sympathetic and cooperative. Finally, the author especially wishes to thank Miss Helen F. Burrus, the department secretary at Caltech, for typing the thesis on the top of a staggering number of other activities.

ABSTRACT

Two existing gravity gradiometers are discussed and a single signal equation is developed for both instruments. Equations are derived for calculating the gradiometer signal from known spherical harmonic coefficients. The result is a signal equation in the same form as the harmonic expansion but with a "gradiometer" polynomial. Next, an integral curvefit procedure is developed for calculating the harmonic coefficients of the gravitational field from known gradiometer data. The procedure only requires calculation of a theoretical observation matrix, thus the orbit determination part of the algorithm is the rate determining step. This increases in cost as the fourth power of the maximum harmonic degree considered. Calculations using parts of the algorithm are discussed and procedures for dealing with error sources are described. Finally, a brief description of a complete gradiometer data reduction program is presented.

TABLE OF CONTENTS

PART	TITLE	PAGE
	ACKNOWLEDGMENT	ii
	ABSTRACT	iii
	TABLE OF CONTENTS	iv
	LIST OF SYMBOLS	vi
	NOTATION AND COORDINATE SYSTEMS	x
I	INTRODUCTION	1
II	THE GRADIOMETER SIGNAL EQUATION	8
	II. 1 Gradiometers Constructed from Accelerometers	9
	II. 2 Mechanical Gradiometers	12
	II. 3 Observations about the Signal Equation	14
	II. 4 Error Sources in the Signal Equation	16
III	THE SIGNAL IN SPHERICAL HARMONICS	20
	III. 1 Derivatives with Respect to Local Satellite Coordinates	21
	III. 2 Evaluation of the Polynomials	25
	III. 3 Relating the Second Derivatives to the Signal Equation	27

TABLE OF CONTENTS (cont'd)

PART	TITLE	PAGE
IV	AN INTEGRAL CURVEFIT TECHNIQUE	32
	IV. 1 Linearization of the Signal Amplitude	33
	IV. 2 Derivation of Integral Curvefit Technique	37
	IV. 3 Expansion of Polynomials in Fourier Series	42
	IV. 4 Weighting Functions	45
	IV. 5 Other Possibilities	47
V	RESULTS AND EVALUATION OF ERROR SOURCES	49
	V. 1 Data on a Sphere	49
	V. 2 Cost of Gradiometer Data Reduction	56
	V. 3 Drifts in the Proportionality Constant	58
	V. 4 Satellite Orientation Errors	60
	V. 5 Orbit Determination Errors	61
	V. 6 Spin Rate Effects	63
	V. 7 The Signal to Noise Ratio	65
VI	AN ALGORITHM FOR GRAVITY GRADIOMETER DATA REDUCTION	66
	VI. 1 Input Data	66
	VI. 2 The Trajectory Calculation	68
	VI. 3 Data Purification	70
	VI. 4 Integral Curvefit Calculations	72
VII	CONCLUSIONS	74
	REFERENCES	77

LIST OF SYMBOLS

- A The transformation matrix relating local coordinates to global coordinates defined by III. 2.
- a A constant defined in Table IV. 2.
- B The transformation matrix relating global coordinates to satellite coordinates defined by III. 13.
- b A constant defined in Table IV. 2.
- b. c. Block center.
- C_{nm} The degree, n , order, m , harmonic coefficient defined by III. 1.
- C_{nm}^i The cosine coefficient for the $\cos i\theta$ term in the Fourier expansion of P_{nm} from Table IV. 2.
- EU Eötvös unit, $1 \text{ EU} = 10^{-9}/\text{sec}^2$.
- G_{nm} Gradiometer polynomial, $G_{nm} = \frac{\partial^2 P_{nm}}{\partial z^2} - \frac{\partial^2 P_{nm}}{\partial x^2}$
- GM The product of the earth's mass and the gravitational constant, a fundamental constant.
- GW_{nm} A gradiometer polynomial times its appropriate weighting function, defined by IV. 16.
- I The arm inertia for the Hughes gradiometer (figure II. 2).
- I_{ij}^c An integral used to determine the degree, i , and order, j , cosine harmonic coefficient. Either IV. 10 or IV. 15 (after IV. 15) define this quantity.
- I_{ij}^s Same as I_{ij}^c except for sine coefficient.
- I_s Rotational inertia of the satellite (figure II. 2).
- i Orbit inclination (figure III. 2).
- i An index in section IV for degree.
- i A unit vector in the local x direction in section II.
- J_n The $C_{n,0}$ harmonic coefficient from III. 1.

- j An index in section IV for order.
- \hat{j} A unit vector in the local y direction in section II.
- K The spring constant of the center spring on the Hughes gradiometer (figure II. 2).
- K_o The spring constant of the two exterior springs on the Hughes gradiometer (figure II. 2).
- \hat{k} A unit vector in the local y direction in section II.
- m The mass of one of the four arm masses for the Hughes gradiometer in section II (figure II. 2).
- m An index for order.
- n An index for degree.
- O The observation matrix defined by IV. 10.
- O_{nji} An element of the observation matrix. See the paragraph that follows IV. 10 for an explanation of the indices.
- O^{-1} Inverse of O .
- P_{nm} The associated Legendre polynomial of degree, n , and order, m , defined by III. 7.
- P_{nm}^{xy} A notation, see note following this section.
- Q The quality factor for the Hughes gradiometer introduced in II. 5. This quantity is experimentally determined by the instrument manufacturer.
- R The equatorial radius of the earth, a fundamental constant.
- r A characteristic radial dimension for a gradiometer in section II, see figures II. 1 and II. 2.
- r The radial position of the satellite in spherical coordinates (figure III. 1).
- S_i The signal from the i -th accelerometer (figure II. 1).
- S_{nm} The degree, n , order, m , harmonic coefficient defined by III. 1.
- S_{nm}^i The sine coefficient for the $\sin i\theta$ term in the Fourier expansion of P_{nm} from Table IV. 2.

t	Time in section II.
t	The argument of a polynomial in section III, $t = \cos = \sin$.
V	The gravitational potential defined by III. 1.
V_{xy}	A notation, see note following this section.
X	Global coordinate defined in figure III. 1.
x	Local coordinate defined in figure III. 1.
Y	Global coordinate defined in figure III. 1.
y	Local coordinate defined in figure III. 1.
Z	Global coordinate defined in figure III. 1.
z	Local coordinate defined in figure III. 1.
Δx	The change in x from figure II. 1.
Δy	The change in y from figure II. 1.
Δz	The change in z from figure II. 1.
θ	The difference in arm deflections for the Hughes gradiometer (figure II. 2). The quantity measured by the Hughes instrument. $\theta = \theta_o - \theta_e$.
θ	The colatitude from section IV, $\theta = \pi - \phi$, from figure III. 1.
θ_o	Deflection of the odd numbered arm from figure II. 2.
θ_e	Deflection of the even numbered arm from figure II. 2.
θ_s	Rotation of the satellite from figure II. 2.
θ_t	Total deflection, $\theta_t = \theta_e + \theta_o$, from figure II. 2.
λ	The longitude of the satellite from figure III. 1.
ν	The true anomaly from figure III. 2.
ϕ	The latitude of the satellite from figure III. 1.
Ω	The right ascension of the node from figure III. 2.

- ω The argument of perigee from figure III. 2 in section III.
- ω The spin rate of the satellite in section II.
- ω_g The resonance frequency of the Hughes gradiometer, $\omega_g = 2\omega$.

NOTATION AND COORDINATE SYSTEMS

P_{nm} is the associated Legendre polynomial defined by III. 7. It differs from P_n^m by $(-1)^m$.

$\binom{n}{m}$ is the binomial coefficient in IV. 13, $\binom{n}{m} = \frac{n!}{(n-m)! m!}$.

V_{xy} , etc. stands for $\frac{\partial^2 V}{\partial x \partial y}$

P_{nm}^{xy} , etc. stands for $\frac{\partial^2 P_{nm}}{\partial x \partial y}$

Quantity $\left| \begin{array}{l} \text{superscript} \\ \text{subscript} \end{array} \right.$ means the quantity is to be evaluated at the location of the subscript and, or identifies the meaning (source) of the quantity in the superscript.

Examples:

$V_{xz} | J_2$ means the term from $\frac{\partial^2 V}{\partial x \partial z}$ with a J_2 coefficient.

$\text{Ampl} |^{meas}$ means the amplitude of the gradiometer data actually measured in a satellite.

$\text{Ampl} |_{orbit}^{meas}$ means the same as $\text{Ampl} |^{meas}$ but specifies the data is taken along the satellite orbit.

Four coordinate systems are being used:

1. local coordinates (x, y, z) from figure III. 1.
2. spherical coordinates (r, λ ,) or (r, λ ,) from figure III. 1.
3. global coordinates (X, Y, Z) from figure III. 1.
4. satellite coordinates from figure III. 2.

I. INTRODUCTION

Observation of the earth is one of the most relevant applications of satellite technology. In this era of skepticism about the space program, weather satellites, communications satellites, and military satellites are unique in that the information they gather has obvious and direct application to the rest of the world. Earth physics satellites are in a similar class. These are satellites that measure properties of the earth itself. Some of the properties of the earth that might be measured using satellites are the variations in the earth's gravitational field, the altitude of the earth's surface, and the ocean's tidal variations. While the relevance of this type of science, known as Geodesy, is not as obvious as that from weather satellites, the applications of Geodesy include areas in Geology, Oceanography and Cartography, as well as satellite orbit determination.

This thesis deals with one of the fundamental quantities in Geodesy: local variations in the earth's gravitational field. Gravitational perturbations are of interest for several reasons. The most obvious application of gravitational data is in the area of orbit determination. Improved representation of the gravitational field is fundamental to improving the accuracy to which satellite trajectories may be determined. Another application is of military interest. A more detailed model of the earth's gravitational field would result in greater precision in the determination of relative positions on the earth's surface. This would have an application in the aiming of Intercontinental Ballistic Missiles.

National Aeronautics and Space Administration is currently studying the applications of satellite technology in Geodesy. The current program plan identifies the need for gravitational data in Oceanography and Geology. Gravitational data coupled with satellite altimetry data would facilitate modeling ocean tides. Gravitational data would help to determine the altimeter satellite trajectory to the required accuracy and also would independently determine the geoid. The difference between geoid height and ocean surface height represents the dynamic head associated with tides, ocean currents, and storm surges. In Geology, measurement of gravitational perturbations is a way of obtaining information about the subsurface structure of the earth. A more detailed gravitational model coupled with existing data might lead to a causal model for the density distribution of the earth with possible applications in mining and earthquake modeling. For a more complete picture of what might be accomplished the reader could refer to the Williamstown report (1) or to the current National Aeronautics and Space Administration plan (2).

This thesis discusses data reduction from a prospective satellite experiment for determination of the earth's gravitational field - a gravity gradiometer experiment. The gravity gradiometer measures a combination of second spatial derivatives of the gravitational potential; i. e., the spatial change in acceleration. The gradiometer accomplishes this by utilizing proof masses to measure the small differences in acceleration between points in the satellite. This quantity is a field variable which can be measured in free-fall, thus the gradiometer is adaptable to a satellite experiment.

There are several reasons why a satellite experiment would be advantageous. The most important advantage of a satellite experiment is that it allows complete, uniform coverage of the earth in a relatively short time span. Ground based geological surveys have already covered most of the land areas of the earth. It is in coverage of the oceans, polar regions, and inaccessible land masses that a satellite study offers an attractive contribution. Another advantage of a satellite experiment is that the local terrain need not be corrected for. In a satellite the nearest topography is several hundred kilometers away. This eliminates the need for terrain corrections. A further advantage of the same sort is that the ambiguity of needing a geoid to determine a geoid is reduced. From a satellite, the measurement is referenced to the local equipotential surface. At satellite altitudes this is a considerably smoother surface than at sea level.

A more technical way of stating these last two advantages is to observe that satellite techniques insure convergence of the spherical harmonic expansion for the earth's gravitational field. Short wave lengths decay rapidly with altitude. Thus, one can treat the field as if it were convergent. On the surface the expansion is very slowly convergent. At satellite altitudes it converges rapidly at wave lengths of the order of the satellite altitude. This is a two sided thing: on one hand, one can't obtain arbitrarily short wave lengths with satellite methods; on the other hand, the gravitational field can be modeled to arbitrary accuracy at satellite altitudes. One of the main advantages of the gradiometer technique when compared to other satellite

techniques is that it extends the range of wave lengths attainable at satellite altitudes.

There are a number of other techniques that have been proposed for obtaining gravitational data. Direct observation of long term satellite motions from the earth has been applied to calculate the gravitational field (3). The data reduction technique used involves expressing the orbital elements as Fourier series whose coefficients are expressed as linear functions of the spherical harmonic coefficients. This is known as frequency decomposition. The accuracy of this technique is expected to improve dramatically in the next few years with the development of laser position determination.

Doppler radar or laser measurement of the range between two satellites has been proposed as a possible experiment for determining the earth's gravitational field (4,5). The range rate between an earth synchronous satellite and a low test satellite could be measured. Alternately, two low test satellites might be used, one continuously ranging the other. A recent proposal for data reduction involves parameter fitting to an assumed mass distribution on the ground (5).

A radar altimeter has been suggested for determination of the earth's gravitational field. Altimetry data alone contains considerable information about the gravitational field in the ocean regions where the mean surface height closely follows the geoid. This information coupled with existing surface data could be used to improve existing representations of the gravitational field (6).

Techniques for ground based gravitational measurements are in a much more refined state. The procedure generally used is

precise measurement of the period of a pendulum. This data is converted to an acceleration and mapped as anomalies over the area surveyed. Characteristically this is done for geological surveys in an attempt to find oil or mineral deposits. Unfortunately, accurate measurements are difficult over water. Use of gradiometers is currently being investigated as a technique applicable to ship or aircraft carried experiments (7) and a data reduction technique has been proposed for reducing horizontal gradients to geoid height (8).

It is within this framework of existing proposals that yet another proposal, the gravity gradiometer satellite, should be considered as a potential satellite experiment. The gradiometer technique offers a number of advantages when compared to more conventional satellite techniques. First, the gradiometer measures a combination of spatial derivatives of acceleration. Differentiation accentuates high frequencies, thus the gradiometer tends to selectively measure the unknown high frequency components of the gravitational field. The other satellite techniques measure lower order derivatives of the field, thus their signals are composed of a larger proportion of low frequencies (9).

Another advantage of the gradiometer technique is that it is relatively insensitive to drag. Atmospheric drag causes changes in a satellite's velocity and position which are an error source for other satellite techniques. However, to the extent that the drag acts uniformly on all parts of the satellite, there is no change in the spatial derivative of acceleration even if the drag varies with time. All the proof masses experience the same deceleration due to drag, thus the

difference in acceleration between points in the satellite is zero regardless of the time history of the measurement.

A final advantage of the gradiometer technique when compared to other satellite techniques is that it makes a direct measurement. The most important consequence of this is that the time history of the measurement is insignificant. Ignoring imperfections in the instrument the gradiometer will read the same irrespective of how it arrived at its current location. Thus a number of different satellites in different trajectories would not significantly improve the accuracy of the measurement except by increasing the amount of data. For this reason the gradiometer lends itself to data reduction techniques more often associated with surface measurements than satellite techniques. At the same time, the gradiometer preserves the satellite advantage of working with a convergent field.

These advantages are achieved at a price, obviously. The gradiometer technique is relatively new and data reduction procedures have not been completely developed for it. Also, there are a number of potential dynamics problems associated with the instrument and its alignment. The frequency resolution and accuracy of the instrument is not as satisfactory as can be achieved with ground based measurements. Finally, there are a host of practical problems associated with carrying the instrument in a satellite. This thesis is directed at one of these problems: the data reduction problem. The intent is to demonstrate that reduction of gradiometer data to the coefficients of the spherical harmonic expansion is both possible and practical.

In the material that follows, the general properties of gradiometers will be discussed. Next an integral formulation of the data reduction problem will be developed. This requires a new set of polynomials based on the derivatives of Legendre polynomials. These polynomials can be orthogonalized with respect to a set of weighting functions. A theoretical procedure will be developed for doing this, thus allowing calculation of the spherical harmonic coefficients without calculation of an experimental observation matrix.

II. THE GRADIOMETER SIGNAL EQUATION

In this section two existing gravity gradiometers will be discussed and a single signal equation will be developed for both instruments.

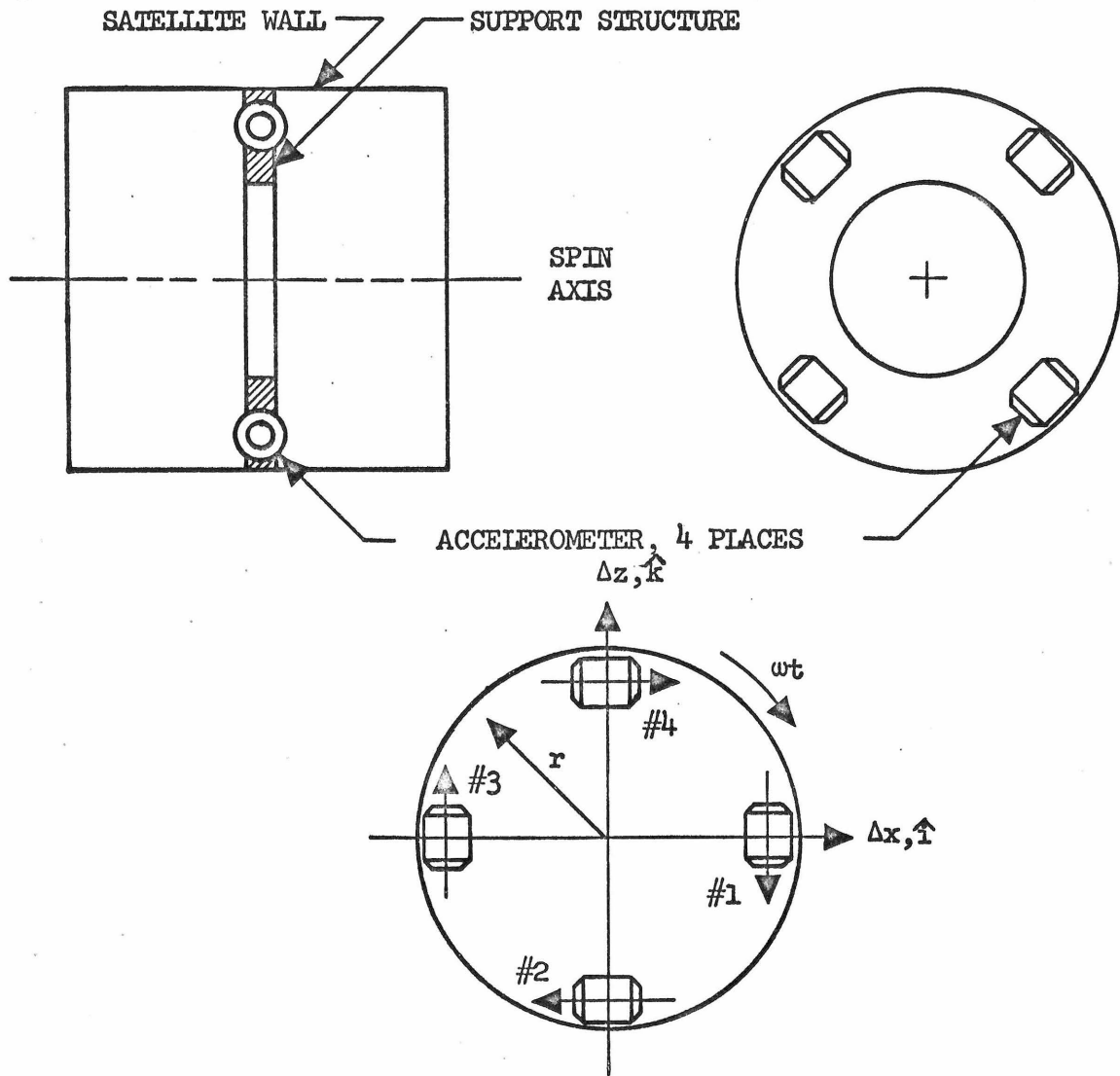
At least two manufacturers are engaged in developing gradiometers suitable for satellite Geodesy applications. They are Bell Aerospace of Buffalo, New York, and Hughes Research of Malibu, California. The Bell Aerospace design calls for four directional accelerometers rigidly attached to the walls of a cylindrical, spin stabilized satellite. The sensitive axis of each accelerometer would be directed tangentially, i. e. the proof masses inside the accelerometers would be constrained radially. The signal from diagonally opposing accelerometers would be added and the pair of resulting signals would be subtracted. The Bell Aerospace accelerometers have been flight qualified and used in several satellite programs in other configurations.

The Hughes design calls for a pair of torsional spring-mass oscillators, composed of two arms in the shape of a cross, with torsional springs cross connecting the arms and connecting the arms to the walls of a spin stabilized satellite. Heavy proof masses would be located on the ends of the arms and the "difference" mode of the resulting spring mass oscillator would be tuned to resonate with the gradient signal. Operational laboratory apparatus has been tested in the case of the Hughes instrument.

II. 1 Gradiometers Constructed from Accelerometers

Taking the proposals one at a time, consider the Bell Aerospace instrument operating at a fixed point in a gravitational field which varies slowly with position. The situation is indicated in Figure II. 1. Think of an accelerometer as a proof mass sliding on a frictionless wire. The proof mass is centered electronically so that a signal is produced which is proportional to the force required to maintain the proof mass at the center of the wire. Thus the signal is proportional to the acceleration relative to the accelerometer housing that the proof mass would experience if free to travel along the sensitive axis. The entire system rotates about the y axis. The acceleration due to this rotation is radial and the sensitive axes are tangential; thus no signal is produced by the satellite rotation.

The situation due to the gravitational field is different, however. Since the field is slowly varying, one is justified in writing a Taylor's series expansion for the gravitational potential. This must be carried to at least second order. By differentiating the Taylor's series expansion with respect to each of the coordinate axes one obtains the vector acceleration of the proof masses as a function of position (x, y, z) . Substituting expressions for sinusoidal motion in the x, z -plane as a function of time, and dotting these expressions with a time variant unit vector in the direction of each accelerometer's sensitive axis (i. e. , taking the vector component of acceleration in the direction of the sensitive axis), one obtains the four equations shown in II. 1 for the signal of each accelerometer.



ACCELERATION:

$$(V_x + V_{xz} \Delta z + V_{xx} \Delta x) \hat{i} + (V_z + V_{xz} \Delta x + V_{zz} \Delta z) \hat{k}$$

POSITION:

SENSITIVE AXIS:

Δx	Δz		\hat{i}	\hat{k}
$r \cos \omega t$	$-r \sin \omega t$	#1	$-\sin \omega t$	$-\cos \omega t$
$-r \sin \omega t$	$-r \cos \omega t$	#2	$-\cos \omega t$	$\sin \omega t$
$-r \cos \omega t$	$r \sin \omega t$	#3	$\sin \omega t$	$\cos \omega t$
$r \sin \omega t$	$r \cos \omega t$	#4	$\cos \omega t$	$-\sin \omega t$

FIGURE II.1 THE BELL AEROSPACE GRAVITY GRADIOMETER

$$S_1 \propto -\sin \omega t V_x - \cos \omega t V_z + r \sin \omega t \cos \omega t (V_{zz} - V_{xx}) - r(\cos^2 \omega t - \sin^2 \omega t) V_{xz}$$

$$S_2 \propto -\cos \omega t V_x + \sin \omega t V_z - r \sin \omega t \cos \omega t (V_{zz} - V_{xx}) + r(\cos^2 \omega t - \sin^2 \omega t) V_{xz}$$

$$S_3 \propto \sin \omega t V_x + \cos \omega t V_z + r \sin \omega t \cos \omega t (V_{zz} - V_{xx}) - r(\cos^2 \omega t - \sin^2 \omega t) V_{xz}$$

$$S_4 \propto \cos \omega t V_x - \sin \omega t V_z - r \sin \omega t \cos \omega t (V_{zz} - V_{xx}) + r(\cos^2 \omega t - \sin^2 \omega t) V_{xz}$$

(II. 1)

The satellite response is just enough to cancel the first order derivatives in equation II. 1 except for satellite drag terms. This is the reason that the signals can not be combined to measure acceleration. However, by adding the signals from diagonally opposing accelerometers and subtracting the resulting pair of signals, one obtains the signal equation for the Bell Aerospace gradiometer.

$$\text{Signal} \propto \sin 2\omega t (V_{zz} - V_{xx}) - 2 \cos 2\omega t V_{xz} \quad (\text{II. 2})$$

Satellite drag can be measured using the same four accelerometers in this configuration. This is done by subtracting opposing pairs of signals and adding the resulting pair of signals. The resulting signal has an amplitude proportional to the in-plane drag and the phase can be used to solve for the direction of the drag.

II.2 Mechanical Gradiometers

Next consider the Hughes instrument operating at a fixed point in the same gravitational field. By balancing the moments of the gradiometer arms, one can show that the ideal equations of motion for the simple three degree of freedom system shown in figure II.2 are:

$$\begin{aligned}
 I\ddot{\theta}_o + K(\theta_o - \theta_e) + K_o(\theta_o - \theta_s) &= mr^2 \{ (V_{zz} - V_{xx}) \sin 2\theta_o - 2V_{xz} \cos 2\theta_o \} \\
 I\ddot{\theta}_e + K(\theta_e - \theta_o) + K_o(\theta_e - \theta_s) &= -mr^2 \{ (V_{zz} - V_{xx}) \sin 2\theta_e - 2V_{xz} \cos 2\theta_e \} \\
 I_s \ddot{\theta}_s + K_o(2\theta_s - \theta_o - \theta_e) &= \text{Drag Torque} \qquad (II.3)
 \end{aligned}$$

Taking the sum and difference of the first two equations one can very nearly separate the difference equation from the other two. Define $\theta = \theta_o - \theta_e$ and $2\theta_t = \theta_o + \theta_e$ where θ is proportional to the strain measured by the Hughes instrument.

$$\begin{aligned}
 I\ddot{\theta} + (2K - K_o)\theta &= 2mr^2 \{ (V_{zz} - V_{xx}) \sin 2\theta_t - 2V_{xz} \cos 2\theta_t \} \cos \theta \\
 2I\ddot{\theta}_t + 2K_o(\theta_t - \theta_s) &= 2mr^2 \{ (V_{zz} - V_{xx}) \cos 2\theta_t + 2V_{xz} \sin 2\theta_t \} \sin \theta \\
 I_s \ddot{\theta}_s + 2K_o(\theta_s - \theta_t) &= \text{Drag Torque} \qquad (II.4)
 \end{aligned}$$

Since the difference between the arm deflections, θ , is very small, the last two equations approach the solution: $\theta_s = \theta_t = \omega t$. Upon introduction of a damping term, $I \omega_g \dot{\theta}/Q$; after defining the

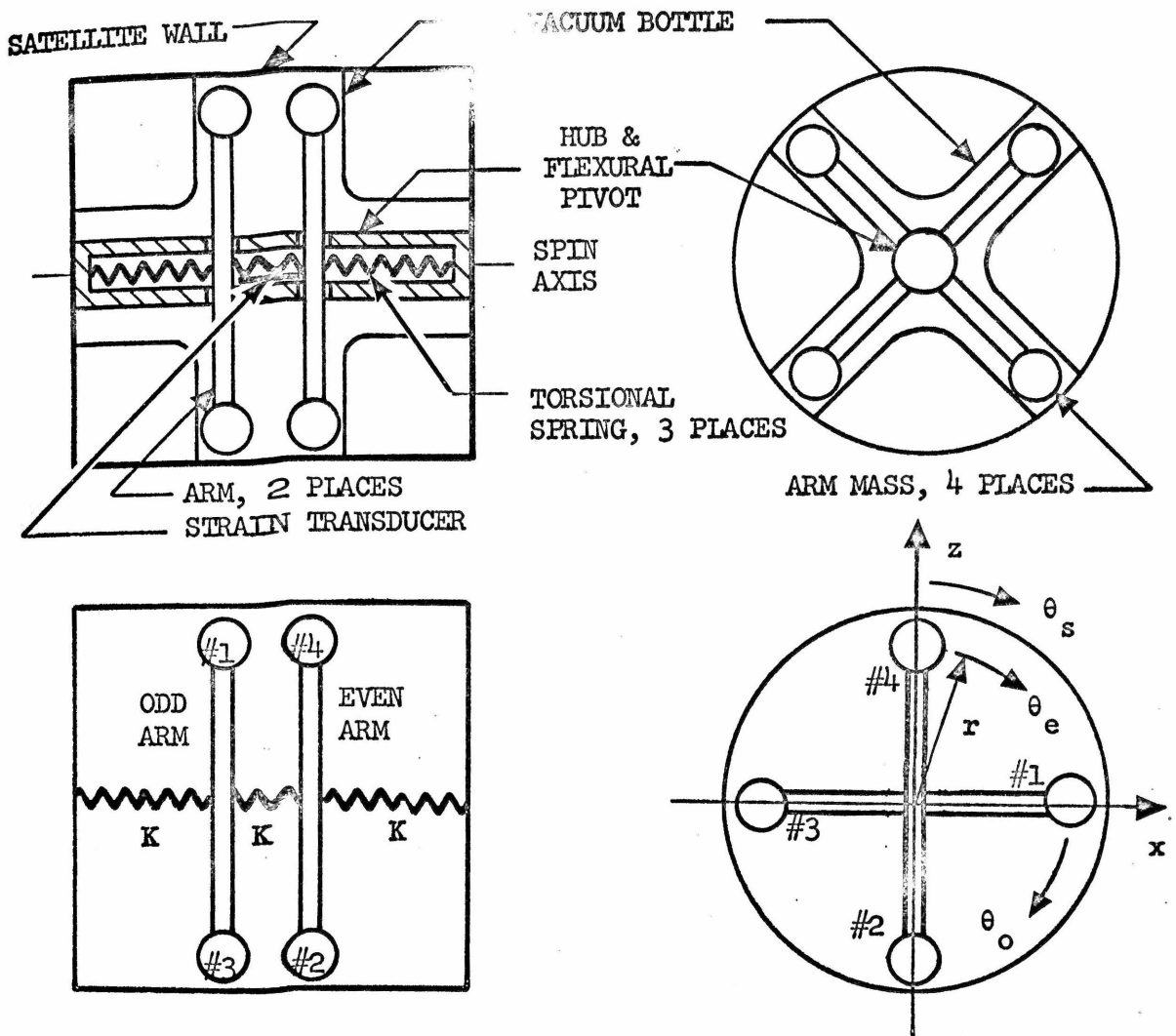


FIGURE II.2 THE HUGHES GRAVITY GRADIOMETER

quantity $\omega_g = (2K - K_o)/I$, the resonance frequency of the sensor; and after observing that $I = 2mr^2$; one obtains equation II. 5.

$$\ddot{\theta} + \frac{\omega_g}{Q} \dot{\theta} + \omega_g^2 \theta = (V_{zz} - V_{xx}) \sin 2\omega t - 2V_{xz} \cos 2\omega t \quad (\text{II. 5})$$

This is the classical harmonic oscillator with a periodic forcing function. Hughes proposes to increase the amplitude of θ by picking the stiffness of the torsional springs such that $\omega_g = 2\omega$. Under this condition, the forcing function on the right is forcing the system at resonance, thus the steady state solution to equation II. 5 is as shown below.

$$\theta = - \frac{Q}{(2\omega)^2} \{ (V_{zz} - V_{xx}) \cos 2\omega t + 2V_{xz} \sin 2\omega t \} \quad (\text{II. 6})$$

The output of the Hughes strain transducer is proportional to this quantity, thus the Hughes output equation is the same as the Bell Aerospace output equation except for a 90° phase shift.

II. 3 Observations about the Signal Equation

There are several points it is important to realize about the gradiometer signal. First, one should realize that the instrument measures a combination of second derivatives of the gravitational potential. It is hoped in this way to extend the range of frequencies that the instrument can measure, and also it is possible to measure this quantity directly in free-fall.

Second, the signal comes at twice spin frequency. This allows separation of the actual signal from a number of noise sources at either nutation frequency or once spin frequency.⁶ From

the derivation it should be clear that the instrument must be rotated to produce a signal, thus a spin stabilized satellite is called for.

Third, the equation is an approximation based on the Taylor's series expansion for the gravitational potential. This is a very good approximation. There are two length scales for the potential: the altitude of the satellite above the surface and the radial distance to the center of the earth. The dimensions of the gradiometer are small compared to either scale.

Fourth, as a consequence of the derivation, the expression involves second derivatives with respect to a spacecraft defined local Cartesian coordinate system. This is unfortunate as an earth centered spherical coordinate system is more natural for gravitational work.

Finally, it is important to realize that both amplitude and phase data are associated with the signal. The amplitude is given by equation II. 7:

$$\text{Amplitude} \propto \sqrt{(V_{zz} - V_{xx})^2 + 4V_{xz}^2} \quad (\text{II. 7})$$

and the phase angle is within an additive constant of equation II. 8.

$$\text{Phase} = \tan^{-1} \frac{2V_{xz}}{V_{zz} - V_{xx}} \quad (\text{II. 8})$$

Both Hughes and Bell Aerospace derive this equation in different ways. By way of comparison the reader could refer to the appropriate proposals by the two companies (10, 11).

II. 4 Error Sources in the Signal Equation

The signal equation is not exact. A number of hardware effects must be considered before one is justified in talking about the signal in this way. Some of the larger errors that must be considered are: 1) long term drifts of the instrument proportionality constant, 2) errors in the orientation of the satellite spin vector, 3) orbital responses to the higher degree terms in the gravitational field, 4) finite spin rate effects, and 5) the instrument signal to noise ratio. These error sources will be discussed in detail in a subsequent chapter (Chapter V) and will only be described here. Another class of at least equally important error sources arises from misalignments of the instrument. These are not within the scope of this thesis.

The signal equation, II. 2, expresses a proportionality between the output signal and the gravitational field. The accuracy of this relationship is limited by the accuracy to which the proportionality constant can be made to hold constant. A number of factors act to change the proportionality constant in orbit. The most important factor will probably be changes in temperature in the satellite. This problem is easily understood in the case of the Hughes instrument. The strain transducer Hughes uses to obtain a readout is functionally dependent on the temperature.

The signal equation is dependent on the orientation of the satellite's spin vector (i. e., the orientation of the x, z-plane with respect to the earth). This orientation can not be maintained precisely. The satellite spin vector tends to rotate in inertial space at a characteristic frequency known as nutation frequency, thus the true

orientation of the spin vector needs to be accounted for in the data reduction. If changes in orientation smaller than the smallest angular position that can be determined caused output signals larger than the instrument significance level, the data could not be corrected. This happens in the case of the angular position with respect to the in-plane rotation, thus the phase angle from equation II.8 can not be measured as accurately as the amplitude can be measured.

The satellite responds to the higher harmonics in the earth's gravitational field. One of the reasons for measuring gravity in the first place is to facilitate prediction of this response, i. e., orbit determination. Obviously this effect must be taken into account in the data reduction procedure. If the error in predicting the response of the satellite were large enough to cause signals of the order of the instrument sensitivity, a simultaneous solution for the satellite response and the gravitational field would be necessary to remove this effect.

The cause of finite spin rate errors can be seen most clearly by considering the differential equation for the Hughes instrument expressing the way the signal is transmitted thru the proof masses (equation II.5 copied below).

$$\ddot{\theta} + \frac{2\omega}{Q} \dot{\theta} + 4\omega^2 \theta = (V_{zz} - V_{xx}) \sin 2\omega t - 2V_{xz} \cos 2\omega t \quad (\text{II.9})$$

Since the satellite translates, $V_{zz} - V_{xx}$ and $2V_{xz}$ can be expressed as periodic functions of time. Further, since the terms on the left are being forced at resonance, the response is highly dependent on the

frequency of the forcing on the right. The product of the spin rate term and any of the frequencies from the terms $V_{zz} - V_{xx}$ and V_{xz} is equal to a sum of sine waves at the sum and difference of the frequencies. If the satellite spin rate, ω , is essentially infinite with respect to the highest frequency of interest there is no problem. For a finite spin frequency the attenuation can be rather large.

The instrument signal to noise level is one of the limiting factors in the design of a gravity gradiometer. Essentially, this problem arises because of Brownian motion of the test masses. This random vibration creates a signal which can not be distinguished from the gradiometer signal. Electrical noise is also a factor. Hughes develops an equation for the signal to noise ratio which can be found in reference 10.

Finally, the reader should be aware of the nature of the misalignment problems mentioned earlier as being outside the scope of this thesis. These occur because of assumptions made in the derivation of the signal equation that can not be met precisely. For example, it was stated in deriving the signal equation for the Bell Aerospace gradiometer that the sensitive axes of the accelerometers were oriented tangentially. This is not possible to arbitrary accuracy. Similarly, the geometric center of the two instruments were both assumed to lie on the spin axis. Again this can not be done to arbitrary accuracy.

Most of these error sources are intimately coupled to the satellite motion, thus it requires an extensive study of satellite motions

to analyze them. In any event, the removal of these errors is expected to occur independently of the rest of the data reduction since the effects are not highly coupled. A series of analyses have been performed in the case of the Hughes instrument, each one concluding that the effects could either be controlled or removed from the data (12, 13 and 14). The instrument sensitivity at which each analysis shows the instrument can operate tends to change between the different studies depending on what sensitivity the dynamicist was asked to verify would work.

III. THE SIGNAL IN SPHERICAL HARMONICS

Equations will be developed for calculation of the gradiometer signal from known spherical harmonic coefficients.

The spherical harmonic expansion for the earth's gravitational field is derived by recognizing that the gravitational field satisfies Laplace's equation in spherical coordinates. By applying separation of variables and requiring continuity at the coordinate boundaries and a zero potential at infinity, one arrives at equation III. 1 for the gravitational field exterior to a sphere of radius R.

$$V(r, \lambda, \phi) = \frac{GM}{r} \sum_{n=0}^{\infty} \left(\frac{R}{r}\right)^n \sum_{m=0}^n P_{nm}(\sin \phi) [C_{nm} \cos m\lambda + S_{nm} \sin m\lambda] \quad (\text{III. 1})$$

The problem with using this representation of the earth's field to represent the output of a gravity gradiometer is that the expressions for the second derivatives with respect to a Cartesian coordinate system are extremely complicated. This is obvious when one considers the chain rule expansion for the second derivative of a function of three variables.

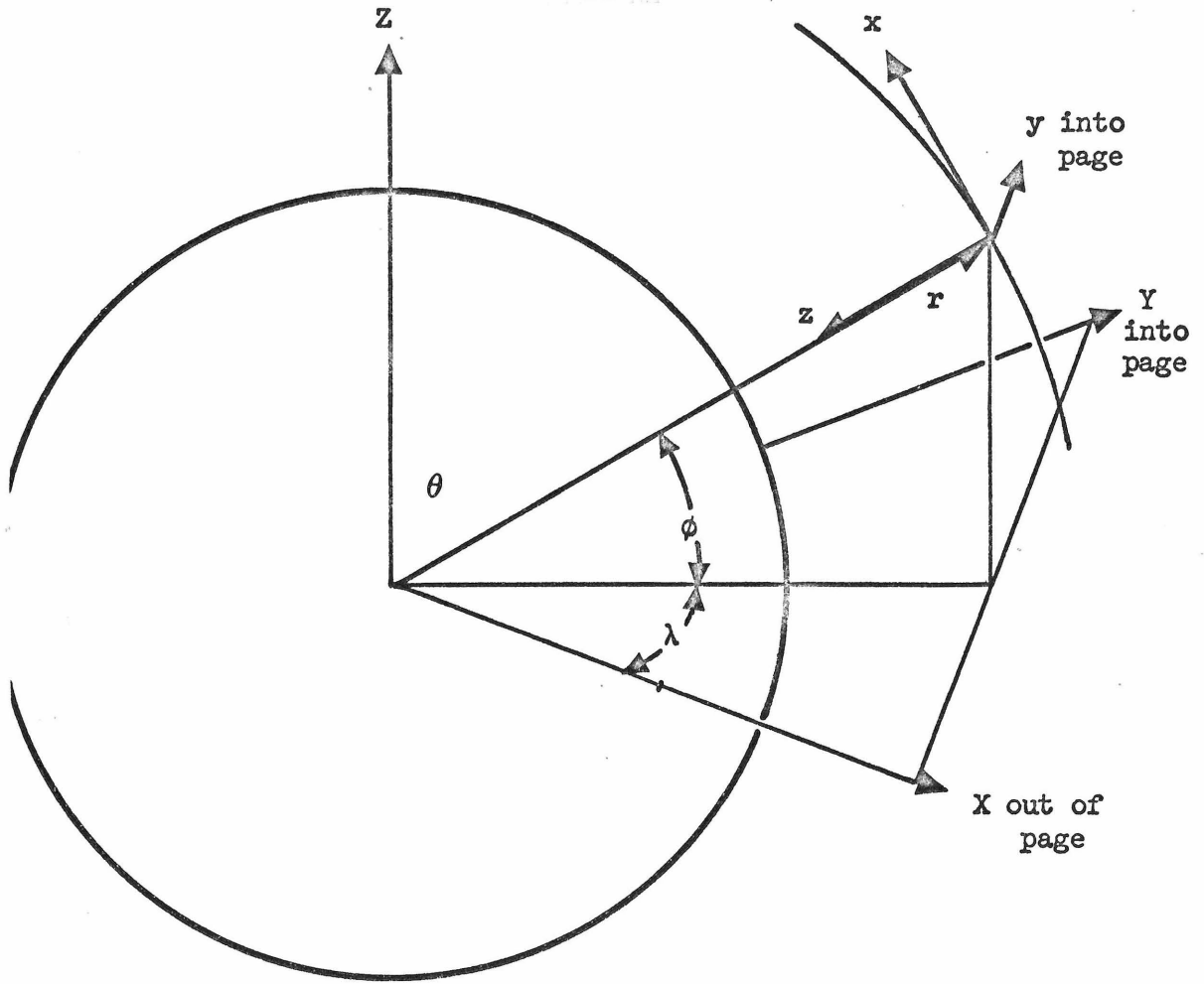
$$\begin{aligned} V_{xx} = & V_{rxx} + V_{\lambda xx} + V_{\phi xx} + V_{rr} r_x^2 + V_{\lambda\lambda} \lambda_x^2 + V_{\phi\phi} \phi_x^2 \\ & + 2(V_{r\lambda} r_x \lambda_x + V_{r\phi} r_x \phi_x + V_{\lambda\phi} \lambda_x \phi_x) \end{aligned} \quad (\text{III. 2})$$

III. 1 Derivatives with Respect to Local Satellite Coordinates

By working at an arbitrary point in space and defining the local x-axis in the direction of ϕ , the latitude; the local y-axis in the direction of λ , the longitude; and the local z-axis in the opposite direction of r , the radius; all but two of the terms in equation III. 2 are identically zero. Figure III. 1 defines this coordinate system. It is necessary to take first and second derivatives of the spherical coordinates with respect to the local coordinates. This requires the transformation between the two coordinate systems. The transformation between global coordinates and the local coordinate system is indicated in equation III. 3.

$$\begin{aligned}
 X &= -\cos \lambda \sin \phi x - \sin \lambda y + \cos \lambda \cos \phi(r - z) \\
 Y &= -\sin \lambda \sin \phi x + \cos \lambda y + \sin \lambda \cos \phi(r - z) \\
 Z &= \cos \phi x + \sin \phi(r - z)
 \end{aligned}
 \tag{III. 3}$$

Working with equation III. 3 and the transformation between global and spherical coordinates, it can be shown that the derivatives of the local coordinates with respect to the spherical coordinates are as shown in Figure III.1. Substituting these expressions into the chain rule expansions for the second derivatives of equation III. 1 with respect to the local coordinates one obtains equations III. 4 and III. 5.



	$\frac{\partial}{\partial x}$	$\frac{\partial}{\partial y}$	$\frac{\partial}{\partial z}$	$\frac{\partial^2}{\partial x^2}$	$\frac{\partial^2}{\partial y^2}$	$\frac{\partial^2}{\partial z^2}$	$\frac{\partial^2}{\partial x \partial y}$	$\frac{\partial^2}{\partial x \partial z}$	$\frac{\partial^2}{\partial y \partial z}$
r	0	0	-1	1/r	1/r	0	0	0	0
λ	0	$\frac{1}{r \cos \phi}$	0	0	0	0	$\frac{\sin \phi}{r^2 \cos^2 \phi}$	0	$\frac{1}{r^2 \cos \phi}$
ϕ	1/r	0	0	0	$\frac{-\sin \phi}{r^2 \cos \phi}$	0	0	1/r ²	0

FIGURE III.1 LOCAL, SPHERICAL, AND GLOBAL COORDINATE SYSTEMS

$$V_{xx}(r, \lambda, \phi) = \frac{GM}{r^3} \sum_{n=0}^{\infty} \left(\frac{R}{r}\right)^n \sum_{m=0}^n P_{nm}^{xx}(\sin \phi) [C_{nm} \cos m\lambda + S_{nm} \sin m\lambda]$$

$$V_{yy}(r, \lambda, \phi) = \frac{GM}{r^3} \sum_{n=0}^{\infty} \left(\frac{R}{r}\right)^n \sum_{m=0}^n P_{nm}^{yy}(\sin \phi) [C_{nm} \cos m\lambda + S_{nm} \sin m\lambda]$$

$$V_{zz}(r, \lambda, \phi) = \frac{GM}{r^3} \sum_{n=0}^{\infty} \left(\frac{R}{r}\right)^n \sum_{m=0}^n P_{nm}^{zz}(\sin \phi) [C_{nm} \cos m\lambda + S_{nm} \sin m\lambda]$$

$$V_{xy}(r, \lambda, \phi) = \frac{GM}{r^3} \sum_{n=0}^{\infty} \left(\frac{R}{r}\right)^n \sum_{m=0}^n P_{nm}^{xy}(\sin \phi) [S_{nm} \cos m\lambda - C_{nm} \sin m\lambda]$$

$$V_{xz}(r, \lambda, \phi) = \frac{GM}{r^3} \sum_{n=0}^{\infty} \left(\frac{R}{r}\right)^n \sum_{m=0}^n P_{nm}^{xz}(\sin \phi) [C_{nm} \cos m\lambda + S_{nm} \sin m\lambda]$$

$$V_{yz}(r, \lambda, \phi) = \frac{GM}{r^3} \sum_{n=0}^{\infty} \left(\frac{R}{r}\right)^n \sum_{m=0}^n P_{nm}^{yz}(\sin \phi) [S_{nm} \cos m\lambda - C_{nm} \sin m\lambda]$$

(III. 4)

where the polynomial expressions are as defined below:

$$\begin{aligned}
P_{nm}^{xx}(\sin \phi) &= \frac{d^2 P_{nm}(\sin \phi)}{d\phi^2} - (n+1) P_{nm}(\sin \phi) \\
P_{nm}^{yy}(\sin \phi) &= - \left(\frac{m^2}{\cos^2 \phi} + (n+1) \right) P_{nm}(\sin \phi) - \frac{\sin \phi}{\cos \phi} \frac{d P_{nm}(\sin \phi)}{d\phi} \\
P_{nm}^{zz}(\sin \phi) &= (n+1)(n+2) P_{nm}(\sin \phi) \\
P_{nm}^{xy}(\sin \phi) &= m \left(\frac{\sin \phi}{\cos^2 \phi} P_{nm}(\sin \phi) + \frac{1}{\cos \phi} \frac{d P_{nm}(\sin \phi)}{d\phi} \right) \\
P_{nm}^{xz}(\sin \phi) &= (n+2) \frac{d P_{nm}(\sin \phi)}{d\phi} \\
P_{nm}^{yz}(\sin \phi) &= m \frac{(n+2)}{\cos \phi} P_{nm}(\sin \phi)
\end{aligned} \tag{III. 5}$$

The equations have been written in this way to emphasize that the form of the spherical harmonic expansion has been preserved. There is a term containing the units, GM/r^3 ; a term expressing altitude variations, $(R/r)^n$; a polynomial in latitude, $P_{nm}^{ij}(\sin \phi)$; and sinusoidal variations in longitude, $\cos m\lambda$ and $\sin m\lambda$. From a dimensional argument one can see that the altitude variations must take this form regardless of the orientation of the local coordinate system. Since the local x direction is perpendicular to the unit vector in the direction of λ and the local y direction is perpendicular to the unit vector in the direction of ϕ , it is obvious that the equations can be written in this form.

III.2 Evaluation of the Polynomials

By applying the chain rule expansion, one can show that the polynomials from equation III. 5 may be written as shown in III. 6 below.

$$\begin{aligned}
 P_{nm}^{xx}(t) &= (1 - t^2) \frac{d^2 P_{nm}(t)}{dt^2} - t \frac{d P_{nm}(t)}{dt} - (n + 1) P_{nm}(t) \\
 P_{nm}^{yy}(t) &= - \left[\left(\frac{m^2}{(1 - t^2)} + (n + 1) \right) P_{nm}(t) + t \frac{d P_{nm}(t)}{dt} \right] \\
 P_{nm}^{zz}(t) &= (n + 1)(n + 2) P_{nm}(t) \\
 P_{nm}^{xy}(t) &= m \left(\frac{t}{(1 - t^2)} P_{nm}(t) + \frac{d P_{nm}(t)}{dt} \right) \\
 P_{nm}^{xz}(t) &= (n + 2)(1 - t^2)^{\frac{1}{2}} \frac{d P_{nm}(t)}{dt} \\
 P_{nm}^{yz}(t) &= m(n + 2)(1 - t^2)^{-\frac{1}{2}} P_{nm}(t)
 \end{aligned} \tag{III. 6}$$

The polynomials in equation III. 6 are always finite. This is not obvious from the form in which they are written, but it follows from substitution of Rodrigues' formula for the associate Legendre polynomial, equation III. 7.

$$P_{nm}(t) = \frac{(1 - t^2)^{m/2}}{2^n n!} \frac{d^{n+m} (t^2 - 1)^n}{dt^{n+m}} \tag{III. 7}$$

Equation III. 4 satisfies Laplace's equation. The sum $P_{nm}^{xx} + P_{nm}^{yy} + P_{nm}^{zz}$ is zero since it is equal to the governing equation for the associated Legendre polynomial, equation III. 8.

$$\frac{d}{dt} \left((1 - t^2) \frac{d P_{nm}(t)}{dt} \right) + \left(n(n + 1) - \frac{m^2}{(1 - t^2)} \right) P_{nm}(t) = 0$$

(III. 8)

From this much information it is possible to calculate the value of the second derivatives at any point using the recursion formulas for the associated Legendre polynomial and the equations just developed for the second derivatives. For example, using Rodriques' formula it can be shown that the first derivative of the associated Legendre polynomial with respect to t is given by equation III. 9.

$$(1 - t^2) \frac{d P_{nm}(t)}{dt} = - n t P_{nm}(t) + (n + m) P_{n-1, m}(t)$$

(III. 9)

Substituting this expression into the governing equation one obtains a three-term recursion relation for the associated Legendre polynomial.

$$(n - m + 1) P_{n+1, m}(t) = (2n + 1) t P_{n, m}(t) - (n + m) P_{n-1, m}(t)$$

(III. 10)

This allows simple calculation of Legendre polynomials and their first derivative. In order to start the procedure, one uses Rodrigues' formula to obtain an expression for the terms of equal order and degree, i. e., $m = n$:

$$P_{mm}(t) = (1 - t^2)^{m/2} \frac{(2m)!}{2^m m!} \quad (\text{III. 11})$$

and the special cases $P_{0,0}(t) = 1$ and $P_{1,0}(t) = t$. Also from Rodrigues' formula it is clear that $P_{nm}(t) = 0$ for m greater than n .

The reader should be warned that equation III. 10 is known as an unstable recursion relation since the coefficient multiplying the terms on the right is larger than unity. The argument here is that any error in P_{nm} will be larger in $P_{n+1,m}$ due to being multiplied by a number larger than one. If the reader is concerned about this, a variety of other recursion relations are available (15).

III. 3 Relating the Second Derivatives to the Signal Equation

At this point it becomes necessary to relate the signal equation (II. 2) to the expressions for the second derivatives (III. 4). This is not as straightforward as it might appear since the orientation of the coordinate system for the signal equation was fixed by the plane of the gradiometer while the coordinate system for the second derivatives was fixed by the location of the gradiometer. In general one of the two coordinate systems must be rotated to the other.

The situation is further complicated by the requirement that the satellite be spin stabilized to provide the necessary rotation for the instrument. Spin stabilization fixes the spin vector in inertial

space not in earth centered space. For normal usage of the gradiometer in a satellite, there is no problem. If the orbit is polar to obtain complete coverage of the earth, and if the spin vector of the satellite is perpendicular to the plane of the orbit, the derivatives of Section III.2 can be substituted directly into the signal equation. If either of these conditions are not met, the derivatives of Section III.2 must be rotated to the coordinate system in which the gradiometer is operating.

In general an Euler angle transformation is required to perform the necessary rotation. First the rotation to inertial space is required. This was already given as equation III.3 repeated as a matrix equation below.

$$\{x_{\text{global}}\} = [A] \{x_{\text{local}}\} \quad (\text{III. 12})$$

Where $[A]$ is:

$$\begin{bmatrix} -\sin\phi \cos\lambda & -\sin\lambda & -\cos\phi \cos\lambda \\ -\sin\phi \sin\lambda & \cos\lambda & -\cos\phi \sin\lambda \\ \cos\phi & 0 & -\sin\phi \end{bmatrix} = \begin{bmatrix} \cos\lambda & -\sin\lambda & 0 \\ \sin\lambda & \cos\lambda & 0 \\ 0 & 0 & 1 \end{bmatrix} \begin{bmatrix} -\sin\phi & 0 & -\cos\phi \\ 0 & 1 & 0 \\ \cos\phi & 0 & -\sin\phi \end{bmatrix}$$

This may be viewed as a rotation of $\phi + 90^\circ$ about the local y-axis followed by a rotation of $-\lambda$ about the global z-axis. The transformation from global to local coordinates is the transpose of this.

Having rotated to global coordinates, the next step is to orient the satellite in the plane of its orbit. To do this the more general Euler angle transformation is required involving the angles: Ω , the

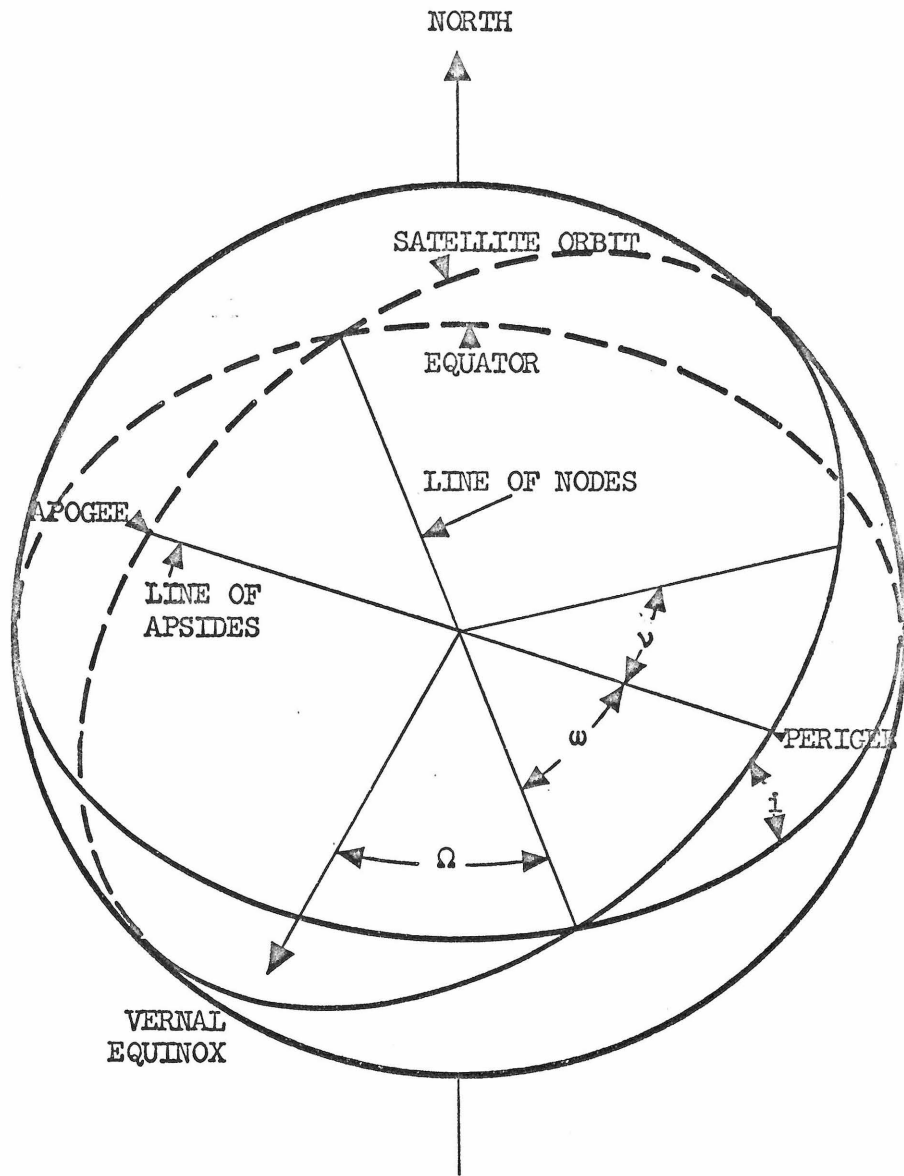


FIGURE III.2 SATELLITE COORDINATE SYSTEM

right ascension of the node; i , the orbit inclination; ω , the argument of perigee; and ν , the true anomaly. This coordinate system is defined in Figure III.2. In general, to orient the y -axis (spin axis) perpendicular to the plane of the orbit, the x -axis in the direction of travel, and the z -axis downward in the radial direction, the transformation defined by equation III. 13 is required.

$$\{x_{\text{satellite}}\} = [B] \{x_{\text{global}}\} \quad (\text{III. 13})$$

Where $[B]$ is:

$$\begin{bmatrix} -\sin(\omega + \nu) & 0 & \cos(\omega + \nu) \\ 0 & 1 & 0 \\ -\cos(\omega + \nu) & 0 & -\sin(\omega + \nu) \end{bmatrix} \begin{bmatrix} 1 & 0 & 0 \\ 0 & \sin i & \cos i \\ 0 & -\cos i & \sin i \end{bmatrix} \begin{bmatrix} \cos \Omega & \sin \Omega & 0 \\ -\sin \Omega & \cos \Omega & 0 \\ 0 & 0 & 1 \end{bmatrix}$$

Thus this transformation may be viewed as a rotation of Ω about the global z -axis, followed by a rotation of $(90^\circ - i)$ about the new x -axis, followed by a rotation of $-((\omega + \nu) + 90^\circ)$ about the new y -axis. This is not a standard Euler angle transformation. Normally one rotates about the z -axis, then the x -axis, and then the z -axis again(16). This series of rotations was used to allow the y -axis to be the spin axis instead of the z -axis. Thus the total rotation for the second derivatives is given by equation III. 14.

$$[V_{ij}^{\text{satellite}}] = [B][A][V_{ij}^{\text{local}}][A^t][B^t] \quad (\text{III. 14})$$

Substituting 0 for ω , ϕ for ν , 90° for i , and λ for Ω , one discovers the transformation is unity. Thus, if a circular polar orbit is used no transformation is required. This of course is what prompted the selection of the coordinate system shown in Figure III. 1 in the first place.

In the preceding transformations it was assumed that the spin vector would be perpendicular to the plane of the orbit. This is not an arbitrary choice. Another alignment would cause the large mean signal to be modulated with the period of the satellite rotation about the earth. This would create several problems. First, the character of the signal would change during different parts of the orbit. At worst the signal would change from small amplitude rather random variations to large amplitude sinusoidal oscillations. The data subsystem would need to be able to handle both cases. Further, phase references would present difficulties. If the spin vector were in the plane of the orbit, the satellite would have to shift between an inertial and an earth centered phase reference to obtain orientation information. Finally, the signal would not be as nearly linear in terms of the harmonic coefficients in any other orientation. Thus there are hardware limitations and data reduction advantages that dictate this choice.

IV. AN INTEGRAL CURVEFIT TECHNIQUE

In this section an integral procedure will be developed for curvefitting the spherical harmonic coefficients of the earth's gravitational field. The procedure under consideration essentially involves a free air reduction of the gradient signal onto the surface of a sphere. This corrected data can be integrated using theoretically derived weighting functions to orthogonalize the data. In order to evaluate the necessary integrals, the signal equation polynomials from equation III.5 will be expanded in Fourier series. This raises the possibility of performing most of the calculations using a fast Fourier transform, thus reducing computer run time.

In proceeding in this way, the data reduction procedure is more like surface data reduction techniques than satellite data reduction techniques. This is made possible because the gradiometer signal amplitude is only a function of position and does not involve initial conditions. The gradiometer satellite is the only gravimetry satellite proposed to date that has this characteristic. The prospects for actually making an integral procedure work are greatly enhanced by the effect of the satellite altitude. Since the satellite is flying well above the surface of the earth, the spherical harmonic expansion is highly convergent at wave lengths shorter than the satellite altitude. Further, global data will be available with the gradiometer satellite. Both of these advantages are not shared by existing surface techniques.

On the other hand, by disregarding the satellite trajectory an error source is introduced which will be highly correlated with the coefficients being calculated. The error due to satellite response to

the higher harmonics is very much like the error in ground based data reduction introduced by not knowing the geoid height. At satellite altitudes this error is considerably reduced for the higher harmonics by the attenuation of the response with altitude. Since the gradiometer measures a higher derivative than the satellite displacement responds to, it is reasonable that a data reduction procedure of this sort will converge at least as fast as surface data reduction procedures based on measuring acceleration.

IV. 1 Linearization of the Signal Amplitude

Since the phase angle of the gradiometer signal can not be measured to the accuracy that the amplitude can be measured, one is constrained to fit data knowing only the signal amplitude. The equation for the signal amplitude is not linear (eq. II. 7 repeated below). This difficulty can be overcome by

$$\text{Amplitude} \propto \sqrt{(V_{zz} - V_{xx})^2 + 4 V_{xz}^2} \quad (\text{IV. 1})$$

recognizing that the signal from the mean earth ($C_{0,0}$) very much dominates the signal. Expanding the signal amplitude equation according to the binomial theorem, one obtains equation IV. 2.

$$\text{Amplitude} \approx (V_{zz} - V_{xx}) + \frac{2 V_{xz}^2}{V_{zz} - V_{xx}} - \frac{2 V_{xz}^4}{(V_{zz} - V_{xx})^3} + \dots \quad (\text{IV. 2})$$

By substituting into equation III. 4 for the derivatives, one can construct a table of estimates for the contributions of the different terms in the expansion above. Table IV. 1 shows these results and

TABLE IV.1 COMPONENTS OF THE GRADIOMETER SIGNAL

COMPONENT	TERM	EXPRESSION	AMPLITUDE AT 100 KM
$C_{0,0} = 1$	$V_{zz} - V_{xx}$	$3 \text{ GM}/r^3 C_{0,0}$	4400 EU
	$2 V_{xz}$	0	0 EU
$J_2 = 0.001083$	$V_{zz} - V_{xx}$	$\frac{\text{GM}}{r^3} \left(\frac{R}{r}\right)^2 \left(\frac{57}{4} \cos 2\theta + \frac{15}{4}\right) J_2$	28 EU
	$2 V_{xz}$	$\frac{\text{GM}}{r^3} \left(\frac{R}{r}\right)^2 12 \sin 2\theta J_2$	18.5 EU
$n \geq 3$ see ref. 9	V_{zz}	$\frac{\text{GM}}{r^3} \sqrt{\sum_n \left(\left(\frac{R}{r}\right)^n (n+1)(n+2) \left(\frac{10^{-5}}{n^2}\right)\right)^2 (2n+1)}$	0.73 EU RMS

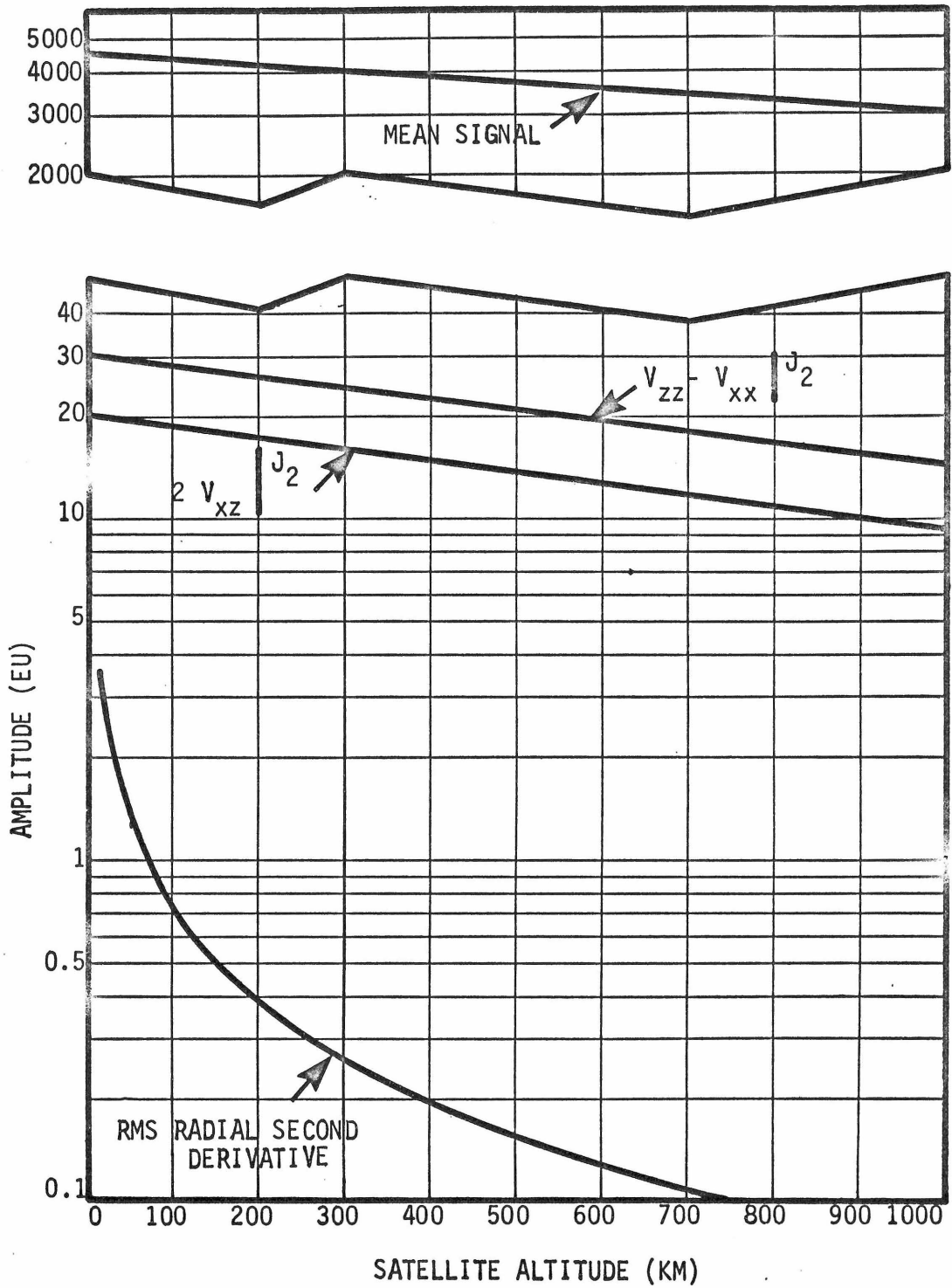


FIGURE IV.1 COMPONENTS OF THE GRADIOMETER SIGNAL VRS ALTITUDE

Figure IV. 1 is a plot of these results as a function of altitude. Using these results one can further simplify equation IV.2. Taking a nominal altitude of 100 km one expects $V_{zz} - V_{xx}$ to have a mean signal larger than 4000 EU (1 EU = $10^{-9}/\text{sec}^2$). The ellipsoidal bulge will contribute less than 30 EU to $V_{zz} - V_{xx}$, and there will be a perturbation signal of about 2 EU RMS. On the other hand, there is no mean contribution to V_{xz} so the ellipsoidal bulge dominates that term with a signal of the order of 20 EU. Again, the perturbation signal to V_{xz} will be relatively small, of the order of 1 to 2 EU RMS.

Substituting these results into equation IV.2, there are a number of possible linearizations depending on how accurately the signal is measured.

$$\text{Amplitude } V_{zz} - V_{xx} \pm \mathcal{O}(0.2 \text{ EU}) \quad (\text{IV. 3})$$

$$\text{Amplitude } V_{zz} - V_{xx} + \frac{2(V_{xz} | J_2)^2}{3 GM/r^3} \pm \mathcal{O}(0.01 \text{ EU}) \quad (\text{IV. 4})$$

$$\text{Amplitude } V_{zz} - V_{xx} - \frac{2(V_{xz} | J_2)^2}{3 GM/r^3} + \frac{4 V_{xz} (V_{xz} | J_2)}{3 GM/r^3} \pm \mathcal{O}(0.0005 \text{ EU}) \quad (\text{IV. 5})$$

In the preceding equations the notation $V_{xz} | J_2$ is intended to imply the term from V_{xz} contributed by the ellipsoidal bulge is to be used alone. The sign change from equation IV.4 to equation IV.5 occurs because the contribution from the ellipsoidal bulge is assumed to be included in the term V_{xz} .

Another linearization procedure is perhaps easier if one considers using the data from a gravity gradiometer to improve the values of an existing reference field. Under this condition one would be able to form an estimate of the amplitude from the reference field using the actual signal amplitude equation (IV.1). If one subtracted the value of $V_{zz} - V_{xx}$ calculated from the reference field from the amplitude calculated from the reference field, the result would be the correction to the actual signal to linearize it so that equation IV.3 held. This has the advantage that the correction is expressed totally in terms of the reference field. Algebraically equation IV.6 illustrates this procedure.

$$V_{zz} - V_{xx} = \text{Ampl} \Big|_{\text{measured}} - (\text{Ampl} \Big|_{\text{ref}} - (V_{zz} - V_{xx}) \Big|_{\text{ref}}) \quad (\text{IV.6})$$

This procedure will have an error of about four times the error in predicting V_{xz} in the reference field times the value of V_{xz} contributed by the ellipsoidal bulge divided by the mean signal amplitude. In any event, this procedure is more accurate than the one implied by equation IV.4 as long as the reference field is at least as complicated as the reference ellipsoid. This linearization procedure was the one used in subsequent calculations.

IV.2 Derivation of Integral Curvefit Technique

One starts to develop the integral curvefit equations by writing down the signal equation and identifying the signal as the actual measured signal.

$$V_{zz} - V_{xx} = \text{Signal}$$

$$\frac{GM}{r^3} \sum_{n=0}^{\infty} \left(\frac{R}{r}\right)^n \sum_{m=0}^n G_{nm}(\phi) (C_{nm} \cos m\lambda + S_{nm} \sin m\lambda) = \text{Signal}(r, \lambda, \phi)$$

$$G_{nm}(\phi) = P_{nm}^{zz} - P_{nm}^{xx} \quad (\text{IV.7})$$

Multiplying on both sides by $G_{ij}(\phi) \cos j\lambda$, requiring r to be constant, and integrating over a sphere of radius, r , one obtains equation IV.8.

$$\begin{aligned} \frac{GM}{r^3} \int_{-\frac{1}{2}\pi}^{\frac{1}{2}\pi} \int_0^{2\pi} \sum_{n=0}^{\infty} \left(\frac{R}{r}\right)^n \sum_{m=0}^n G_{nm}(\phi) G_{ij}(\phi) (C_{nm} \cos m\lambda + S_{nm} \sin m\lambda) \\ \cos j\lambda \cos \phi r^2 d\lambda d\phi = \int_{-\frac{1}{2}\pi}^{\frac{1}{2}\pi} \int_0^{2\pi} \text{Signal} G_{ij}(\phi) \cos j\lambda \cos \phi r^2 d\lambda d\phi \end{aligned} \quad (\text{IV.8})$$

Next one formally interchanges the order of integration and summation. Since sines and cosines are orthogonal one can drop the summation over m , replace m by j , and integrate with respect to λ .

$$\begin{aligned} \pi r^2 \frac{GM}{r^3} \sum_{n=0}^{\infty} \left(\frac{R}{r}\right)^n C_{nj} \int_{-\frac{1}{2}\pi}^{\frac{1}{2}\pi} G_{nm}(\phi) G_{ij}(\phi) \cos \phi d\phi \\ = \int_{-\frac{1}{2}\pi}^{\frac{1}{2}\pi} \int_0^{2\pi} \text{Signal} G_{ij}(\phi) \cos j\lambda \cos \phi r^2 d\lambda d\phi \end{aligned} \quad (\text{IV.9})$$

Realizing that the integral remaining on the left side is just a number, what is left is an equation relating the coefficients of the theoretical expansion to the actual signal. This is the C_{ij} -th equation. Replacing the $\cos j\lambda$ by a $\sin j\lambda$ and repeating the process, one can obtain a similar S_{ij} -th equation. Conceptually, repeating the process over all i and j one has an equation for each coefficient.

$$C_{jj} O_{jji} + \dots + C_{nj} O_{nji} + \dots = I_{ij}^c$$

and
$$S_{jj} O_{jji} + \dots + S_{nj} O_{nji} + \dots = I_{ij}^s$$

where:
$$O_{nji} = \pi r^2 \frac{GM}{r^3} \left(\frac{R}{r}\right)^n \int_{-\frac{1}{2}\pi}^{\frac{1}{2}\pi} G_{nj}(\phi) G_{ij}(\phi) \cos\phi \, d\phi$$

$$I_{ij}^c = \int_{-\frac{1}{2}\pi}^{\frac{1}{2}\pi} \int_0^{2\pi} \text{Signal}(r, \lambda, \phi) G_{ij}(\phi) \cos j\lambda \cos\phi r^2 \, d\lambda \, d\phi$$

$$I_{ij}^s = \int_{-\frac{1}{2}\pi}^{\frac{1}{2}\pi} \int_0^{2\pi} \text{Signal}(r, \lambda, \phi) G_{ij}(\phi) \sin j\lambda \cos\phi r^2 \, d\lambda \, d\phi$$

(IV. 10)

A word on notation is in order here. The use of three indices instead of four in the previous equation is confusing. The notation O_{nji} is intended to imply the coefficient relating the C_{nj} harmonic to the C_{ij} harmonic is being worked with. The coefficients relating the C_{nm} harmonic to the C_{ij} harmonic for $m \neq j$ are all zero. They were eliminated when the $\cos m\lambda$ and $\cos j\lambda$ terms were

found to be zero due to orthogonality in equation IV.9. The resulting matrix of coefficients is indicated in Figure IV.2 for a system truncated at $n = 5$. It will be shown in the next section that only coefficients of the same parity in n and i (i.e., n even and i even or n odd and i odd) are non zero. This accounts for the arrangement of the variables.

At this point one is dealing with a matrix composed only of theoretical quantities on the left and a fairly complicated column vector of integrals of the real signal (mapped on a sphere) on the right. The system looks as follows:

$$\begin{aligned} \begin{bmatrix} O_{nji} \end{bmatrix} \{C_{nj}\} &= \{I_{ij}^c\} \\ \begin{bmatrix} O_{nji} \end{bmatrix} \{S_{nj}\} &= \{I_{ij}^s\} \end{aligned} \tag{IV.11}$$

If the system is non-singular, it can be solved for the coefficients by inverting the observation matrix and multiplying on the right. Experimentally the author has shown the system is non singular, i.e., each non-zero partition has a finite determinant which can be made as large as desired by scaling. Further, the size of matrix that needs to be inverted is small. Inverting by partitions, the largest matrix that needs to be inverted has a dimension of about $n/2$. Since the system converges, i.e., the integrals on the right become negligibly small, the infinite system of equations developed here can be truncated at wave lengths about equal to the altitude the satellite flies at. This is a solvable system of equations.

	n	0	2	4	1	3	5	1	3	5	2	4	2	4	3	5	3	5	4	4	5	5	
n	m	0	0	0	0	0	0	1	1	1	1	1	2	2	2	2	3	3	3	4	4	5	5
0	0	x	x	x																			
2	0	x	x	x																			
4	0	x	x	x																			
1	0				x	x	x																
3	0				x	x	x																
5	0				x	x	x																
1	1							x	x	x													
3	1							x	x	x													
5	1							x	x	x													
2	1										x	x											
4	1										x	x											
2	2												x	x									
4	2												x	x									
3	2														x	x							
5	2														x	x							
3	3																x	x					
5	3																x	x					
4	3																		x				
4	4																			x			
5	4																				x		
5	5																						x

x signifies a non-zero number

FIGURE IV.2 FORM OF THE OBSERVATION MATRIX
TRUNCATED AT DEGREE FIVE

IV.3 Expansion of Polynomials in Fourier Series

The construction of the observation matrix requires expansion of the theoretical integrals from equation IV.10. This is readily accomplished if one observes that the polynomials have a simple expansion in terms of a Fourier series. Returning to equation III.5 one discovers that the polynomials may be represented as shown in equation IV.12.

$$G_{nm}(\phi) = P_{nm}^{zz} - P_{nm}^{xx} = (n+1)(n+3) P_{nm}(\sin\phi) - \frac{d^2 P_{nm}(\sin\phi)}{d\phi^2} \quad (\text{IV.12})$$

The associated Legendre polynomials have a Fourier series which terminates with the term $n\phi$. Further, if one converts to colatitude, θ , instead of latitude, ϕ , (where $\theta = \pi - \phi$) the Fourier series expansions have the properties shown in Table IV.2.

The coefficients of the Fourier series expansion are readily calculated from the recursion relations discussed in Section III.2 by calculating a new recursion relation for the coefficients of the Fourier series expansion. This is done by substituting the Fourier series expansion into the recursion relation and equating amplitudes of frequencies. The results of this operation are shown in Table IV.2 for the recursion relation indicated in equation III.10.

The procedure may be started by the use of the formula shown below.

TABLE IV.2 FOURIER SERIES OF ASSOCIATED LEGENDRE POLYNOMIALS

n	m	FOURIER SERIES EXPANSION	RECURSION RELATION
even	even	even cosine series	$C_{nm}^j = a (C_{n-1,m}^j + C_{n-1,m}^{j-2}) - b C_{n-2,m}^j$
odd	even	odd cosine series	$C_{nm}^j = a (C_{n-1,m}^j + C_{n-1,m}^{j+2}) - b C_{n-2,m}^j$
even	odd	even sine series	$S_{nm}^j = a (S_{n-1,m}^j + S_{n-1,m}^{j+2}) - b S_{n-2,m}^j$
odd	odd	odd sine series	$S_{nm}^j = a (S_{n-1,m}^j + S_{n-1,m}^{j-2}) - b S_{n-2,m}^j$

where: $a = \frac{n - \frac{1}{2}}{n - m}$

$b = \frac{n + m - 1}{n - m}$

$$P_{nm}(\cos \theta) = \frac{C_{nm}^0}{2} + \sum_{j=1}^n C_{nm}^j \cos j\theta + S_{nm}^j \sin j\theta$$

$$\begin{aligned}
P_{mm}(\theta) &= \frac{(2m)!}{2^{2m-1}m!} \left[\frac{1}{2} \binom{m}{m/2} + \sum_{j=1}^{m/2} (-1)^j \binom{m}{\frac{m}{2} - j} \cos 2j\theta \right] \quad m \text{ even} \\
&= \frac{(2m)!}{2^{2m-1}m!} \left[\sum_{j=0}^{\frac{m-1}{2}} (-1)^j \binom{m}{\frac{m-1}{2} - j} \sin(2j+1)\theta \right] \quad m \text{ odd}
\end{aligned}$$

(IV. 13)

This relation is readily obtained from equation III. 11 and the elementary properties of sines and cosines.

Once the expansion for a given associated Legendre polynomial has been calculated, it is extremely easy to calculate the expansion for the polynomial that occurs in the gradiometer signal equation. Returning to equation IV. 12 and converting to colatitude, one obtains equation IV. 14.

$$G_{nm}(\theta) = (n+1)(n+3) P_{nm}(\cos \theta) - \frac{d^2 P_{nm}(\cos \theta)}{d\theta^2} \quad \text{(IV. 14)}$$

$$\begin{aligned}
G_{nm}(\theta) &= (n+1)(n+3) C_{nm}^0 / 2 + \sum_{j=1}^n [(n+1)(n+3) + j^2] \\
&\quad [C_{nm}^j \cos j\theta + S_{nm}^j \sin j\theta]
\end{aligned}$$

This offers a practical method for the calculation of the expansion of the polynomials. It also makes it clear that the properties of the polynomials are much the same as the properties of the associated Legendre polynomials. In particular, the Fourier series expansions of the gradiometer polynomials are in precisely the same form as the

corresponding Fourier series expansions of the associated Legendre polynomials. Thus Table IV.2 applies to the gradiometer polynomials as well as the Legendre polynomials except for the recursion relations.

Having represented the gradiometer polynomials by Fourier series, the integrals of section IV.2 are trivial to integrate. Further, it is obvious that the integral of $G_{nj}(\theta)G_{ij}(\theta) \sin \theta$ over the range zero to pi is zero if the parity of n and i is different. Term by term the parity of the corresponding series is also different. Thus, the even and odd terms separate in the observation matrix as was illustrated in Figure IV.2.

IV.4 Weighting Functions

The process about to be advanced for calculating weighting functions is based on a matrix inversion, thus much of the utility of the weighting function approach is lost. Still the existence of these functions is of major theoretical significance in that the coefficients of the spherical harmonic expansion calculated through this procedure may be viewed as statistically independent due to the orthogonality of the system. Further, practical calculations are simplified.

The first step in calculating a system of weighting functions for the truncated series is to construct and invert the observation matrix for the system. Multiplying this inverse through on both sides of equation IV.11, one obtains an equation that might be considered as the solution to the problem. However, if one observes that the matrix O^{-1} is just a set of numbers, one can conceptually multiply out the matrix multiplication on a term by term basis. The result is a column matrix of sums of integrals. The numbers from the O^{-1} matrix can be

taken inside these integrals and the result for each row can be written under a single pair of integral signs. At this stage each term of the column matrix looks as shown in equation IV. 15:

$$I_{ij}^c = \int_0^\pi \int_0^{2\pi} \text{Signal}(r, \lambda, \theta) (0_{iji}^{-1} G_{ij}(\theta) + \dots + 0_{nji}^{-1} G_{nj}(\theta) + \dots) \cos j\lambda \sin\theta r^2 d\lambda d\theta \quad (\text{IV. 15})$$

If one further considers the polynomials $G_{nm}(\theta)$ as being represented by their Fourier series, one discovers that the resulting polynomial, GW_{nm} , is easily represented as a Fourier series composed of the sums of the Fourier series of $G_{nm}(\theta)$ multiplied by the elements of the inverse of the observation matrix. Thus the polynomials GW_{nm} can be formed independent of reducing the data by matrix multiplying the inverse of the observation matrix times the matrix of Fourier coefficients of the gradiometer polynomials. The system now looks as follows:

$$\begin{aligned} \{C_{nm}\} &= \{I_{nm}^c\} \\ \{S_{nm}\} &= \{I_{nm}^s\} \\ \text{where: } \{I_{nm}^c\} &= \int_0^\pi \int_0^{2\pi} \text{Signal}(r, \lambda, \theta) GW_{nm}(\theta) \cos m\lambda \sin\theta r^2 d\lambda d\theta \\ \{I_{nm}^s\} &= \int_0^\pi \int_0^{2\pi} \text{Signal}(r, \lambda, \theta) GW_{nm}(\theta) \sin m\lambda \sin\theta r^2 d\lambda d\theta \\ \{GW_{nm}\} &= [0^{-1}] [C_{nm}^j] \begin{cases} \frac{1}{2} \\ \cos \theta \\ \vdots \end{cases} \quad m \text{ even} \\ \{GW_{nm}\} &= [0^{-1}] [S_{nm}^j] \begin{cases} \sin \theta \\ \vdots \end{cases} \quad m \text{ odd} \end{aligned} \quad (\text{IV. 16})$$

By comparing this result with the result obtained by multiplying through by a system of weighting functions, one sees that the Fourier series GW_{nm} are just expansions for the products of weighting functions times the gradiometer polynomials. Thus, the weighting function itself is easily found at any value of θ by dividing the value GW_{nm} by the value of G_{nm} at that point. As the system of equations becomes larger the number of terms in the expansion for GW_{nm} becomes larger. In the limit as n goes to infinity the weighting functions stop being band limited functions.

IV.5 Other Possibilities

Practical evaluation of the integrals of equation IV.16 would be facilitated by expanding the signal as a two dimensional Fourier series in λ and θ . This procedure would save computer time if the highly efficient fast Fourier transform can be used. If this is done, the integrals of equation IV.16 are trivial, having effectively been replaced by the correct fast Fourier transform. The author did not have the correct finite fast Fourier transforms (ranges 0 to π and 0 to 2π) available so this obvious simplification wasn't used.

Minor modifications are possible to the basic algorithm advanced above. First, the $\cos \phi$ or $\sin \theta$ term can be completely dropped. The resulting equations will expand the $\sin \theta$ term in a Fourier series as part of GW_{nm} if the term is really doing anything. The equations are faster to integrate without it.

Along the same line of reasoning, it is obvious that any arbitrary surface can be used to integrate over by substituting the

appropriate Fourier expansion for the area element. Thus the integral could be carried out on a reference sphere or a reference ellipsoid. It might even be possible to use a close approximation to a real satellite trajectory though this would vastly complicate the integration.

Also one might use a P_{nm} instead of a G_{nm} when one multiplies the signal equation by the polynomials in equation IV.8. Clearly this would work just as well and one might have large parts of the algorithm already programmed if this were done. Effectively one would be expanding the gradiometer signal in a spherical harmonic series and converting the coefficients of this series to the coefficients for the potential.

Finally, a question may arise as to the uniqueness or completeness of the polynomials, G_{nm} . By uniqueness it is meant that the polynomials are not linear combinations of each other. By completeness it is meant that arbitrary functions can be expanded in a linear combination of G_{nm} 's. The G_{nm} polynomials must be unique since differentiation is unique and the polynomials, P_{nm} are unique. It is not at all clear that the G_{nm} are complete. This makes no practical difference since the field can be represented by the spherical harmonic expansion and the derivatives are uniquely determined from the spherical harmonic expansion. Thus, the gradiometer signal from any field satisfying Laplace's equation can be expanded in this way. Since the inverse is linear and only has one solution, it is clear that the solution is the real gravitational field. In this sense the polynomials G_{nm} are complete. Unfortunately only truncated systems can be dealt with in this way.

V. RESULTS AND EVALUATION OF ERROR SOURCES

In this section some results of calculations using the theory just described will be discussed and procedures for dealing with signal errors will be described.

The theoretical calculations just discussed have been programmed on a Univac 1108 computer using FORTRAN V. The computer was primarily used as a numerical check on the algebra and as a discipline to find the easiest procedure; however in the final stages of development some calculations of general interest were made.

V.1 Data on a Sphere

The reduction of linearized gradiometer data mapped on a sphere to the spherical harmonic coefficients was checked for a reduced size case. Observation matrices were constructed through harmonic order and degree 36. This was done using the technique described in Section IV but without the $\sin \theta$ weighting function. The normalized matrix was inverted, rescaled, and multiplied through the Fourier series expansions for the gradiometer polynomials. The technique described in Section III.2 was used to generate sample data over the entire globe in the center of 5° blocks at a constant altitude of 830 Km. A trapezoid rule integration procedure was used to evaluate the integrals of equation IV.16 and coefficients were recovered in this way. Next the simulated data was truncated to 0.01 EU accuracy and the procedure was repeated.

This procedure was chosen to simulate what would be expected to happen using real satellite data. In reference 17 it is argued that the parameters governing a gradiometer satellite mission are the

satellite altitude and the gradiometer sensitivity. All the other mission design parameters can be computed from these two variables, i. e. digitization rate, block size, spin rate, etc. Even the satellite altitude is fixed to some extent. Given a minimum altitude, one should proceed to the next highest satellite resonance to obtain repeating ground tracks at the correct spacing.

At the normal altitude a gradiometer would fly (200 to 300 km), data reduction based on this procedure would be rather expensive and the data for a simulation would have to be complete to about degree and order 120 (see Figure V. 1). Thus a full scale simulation could not be attempted. The next best thing was done by arbitrarily moving the satellite higher. 830 km was selected because it was expected that a simulation with harmonic degree 36 would converge at a sensitivity of 0.01 EU at that altitude and because it is a satellite resonance altitude with 99 complete, independent passes between repetitions of the ground tracks.

The belief that the data from a gradiometer satellite at 830 km altitude will not contain significant amplitudes from harmonics higher than 36 is supported by the results of calculating the RMS amplitude contributions of the degree sums as described in reference 9. In Figure V. 1 the RMS sum of all the harmonics above and including each degree is plotted using Kaula's rule of thumb. The theoretical calculations, based on twice the radial second derivative, gave a reasonable estimate for the RMS amplitude of the tabular data.

Unfortunately the author did not take his analysis seriously enough and rounded the block size to 5° instead of the 3.75° blocks

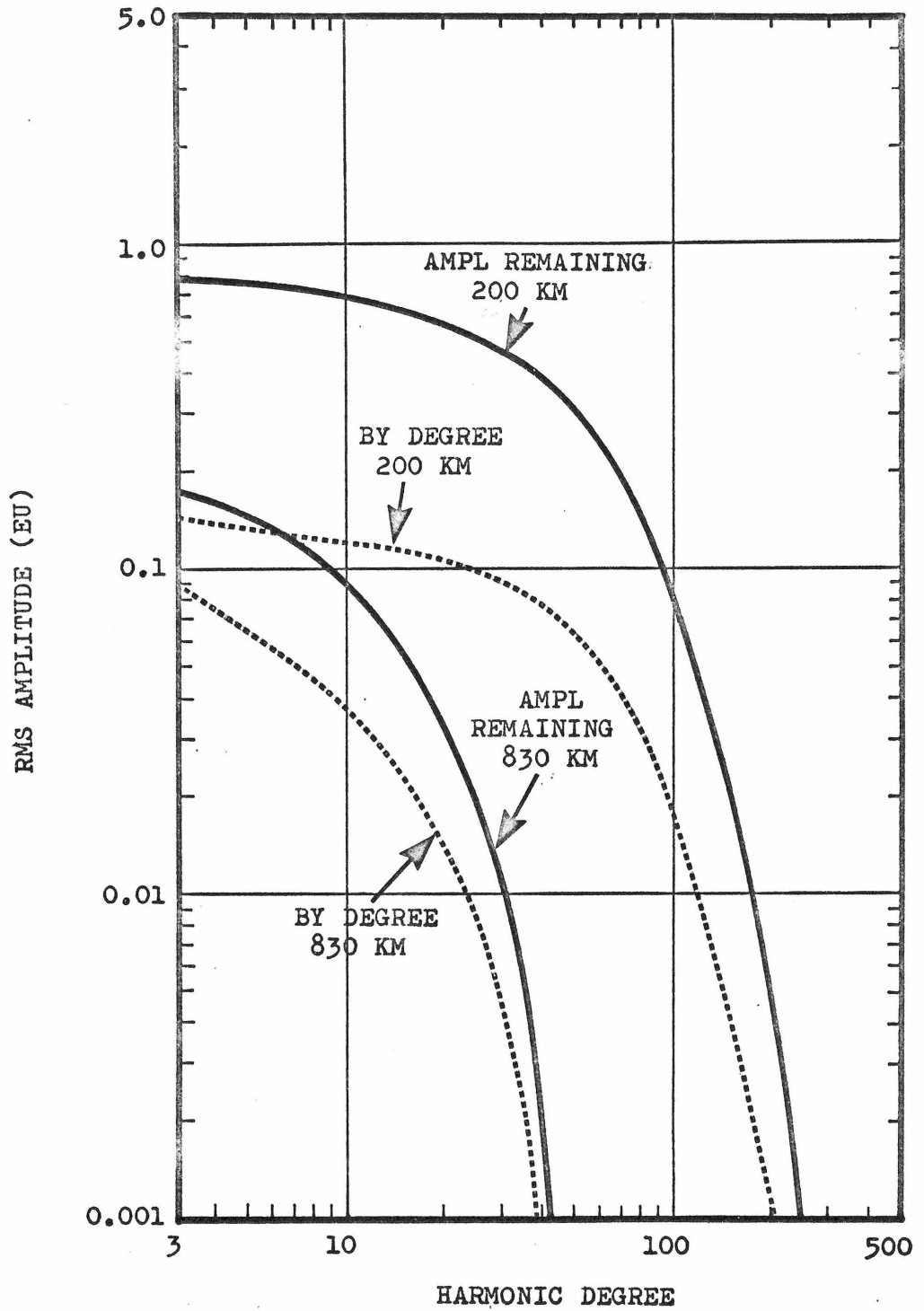


FIGURE V.1 GRADIOMETER AMPLITUDE REMAINING BY HARMONIC DEGREE AND ALTITUDE

required by the approximation that the wave length equal to the altitude is completely attenuated. As a result, most of the errors observed occurred because of integrating the data over finite blocks. When the signal was also attenuated to 0.01 EU only small errors were introduced by comparison. These results are indicated in Table V.1 where selected degrees and orders of coefficients are compared at each step in the analysis.

The results of this demonstration are embarassingly accurate. The errors observed are small when compared to those the author predicted in reference 17. This is not a complete simulation or an error analysis. The accuracy would not hold up at the level reported here in the presence of correlated errors. Random errors shouldn't make much difference since they will tend to average out. The author believes the analysis from reference 17 is still fundamentally sound but must be applied with considerable rigor to maximize the usefulness of the data.

The relative size of the on and off diagonals of the observation matrix is of interest. This is because it indicates how errors in the data would be coupled if the observation matrix were to be constructed and inverted experimentally. Two of the leading partitions of the observation matrix are illustrated in Table V.2. The diagonal has been normalized to one for this table and a sine weighting function was not included. Clearly the coupling is relatively small.

It should be observed that the satellite altitude makes no difference in the matrix when it is normalized in this way. First the variable is redefined as the harmonic coefficient times $(R/r)^n$. Then

TABLE V.1 COSINE COEFFICIENTS CALCULATED BY THE TECHNIQUE

n	m	SIMULATION VALUE	NO TRUNCATION	WITH TRUNCATION
3	0	0.2689 x 10 ⁻⁵	0.2689 x 10 ⁻⁵	0.2691 x 10 ⁻⁵
3	1	0.2104 x 10 ⁻⁵	0.2271 x 10 ⁻⁵	0.2273 x 10 ⁻⁵
3	2	0.3048 x 10 ⁻⁶	0.3351 x 10 ⁻⁶	0.3338 x 10 ⁻⁶
3	3	0.9206 x 10 ⁻⁷	0.9201 x 10 ⁻⁷	0.9147 x 10 ⁻⁷
4	0	0.2371 x 10 ⁻⁵	0.2365 x 10 ⁻⁵	0.2371 x 10 ⁻⁵
4	1	-.5181 x 10 ⁻⁶	-.5549 x 10 ⁻⁶	-.5564 x 10 ⁻⁶
4	2	0.7770 x 10 ⁻⁷	0.1003 x 10 ⁻⁶	0.1003 x 10 ⁻⁶
4	3	0.5732 x 10 ⁻⁷	0.6132 x 10 ⁻⁷	0.6155 x 10 ⁻⁷
4	4	-.1713 x 10 ⁻⁸	-.1722 x 10 ⁻⁸	-.1816 x 10 ⁻⁸
15	0	0.2106 x 10 ⁻⁶	0.2133 x 10 ⁻⁶	0.2124 x 10 ⁻⁶
15	1	0.1546 x 10 ⁻⁷	0.4661 x 10 ⁻⁷	0.4672 x 10 ⁻⁷
15	2	-.1326 x 10 ⁻⁹	0.6014 x 10 ⁻⁹	0.6618 x 10 ⁻⁹
15	3	-.3784 x 10 ⁻¹⁰	-.4518 x 10 ⁻¹⁰	-.4806 x 10 ⁻¹⁰
15	4	0.1521 x 10 ⁻¹¹	0.7070 x 10 ⁻¹²	0.6296 x 10 ⁻¹²
15	5	0.4963 x 10 ⁻¹²	0.5500 x 10 ⁻¹²	0.5547 x 10 ⁻¹²
15	6	0.1239 x 10 ⁻¹³	0.9053 x 10 ⁻¹⁴	0.9322 x 10 ⁻¹⁴
15	7	0.6315 x 10 ⁻¹⁵	0.6008 x 10 ⁻¹⁵	0.5739 x 10 ⁻¹⁵
15	8	-.1703 x 10 ⁻¹⁵	-.1786 x 10 ⁻¹⁵	-.1777 x 10 ⁻¹⁵
15	9	0.7635 x 10 ⁻¹⁸	-.1131 x 10 ⁻¹⁷	-.9321 x 10 ⁻¹⁸
15	10	0.4273 x 10 ⁻¹⁸	0.4722 x 10 ⁻¹⁸	0.4672 x 10 ⁻¹⁸
15	11	0.2202 x 10 ⁻²⁰	-.6231 x 10 ⁻²¹	0.1239 x 10 ⁻²⁰
15	12	-.3366 x 10 ⁻²⁰	-.3640 x 10 ⁻²⁰	-.3819 x 10 ⁻²⁰
15	13	-.5896 x 10 ⁻²¹	-.6086 x 10 ⁻²¹	-.6271 x 10 ⁻²¹
15	14	-.4068 x 10 ⁻²²	-.4195 x 10 ⁻²²	-.4503 x 10 ⁻²²
15	15	-.2415 x 10 ⁻²²	-.2403 x 10 ⁻²²	-.2363 x 10 ⁻²²

Simulation coefficients from reference 18.

TABLE V.1, CONTINUED

n	m	SIMULATION VALUE		NO TRUNCATION		WITH TRUNCATION	
7	7	0.1071	$\times 10^{-11}$	0.1048	$\times 10^{-11}$	0.1068	$\times 10^{-11}$
8	7	-.1487	$\times 10^{-12}$	-.1472	$\times 10^{-12}$	-.1421	$\times 10^{-12}$
9	7	-.1638	$\times 10^{-12}$	-.1702	$\times 10^{-12}$	-.1710	$\times 10^{-12}$
10	7	0.6173	$\times 10^{-13}$	0.6096	$\times 10^{-13}$	0.6191	$\times 10^{-13}$
11	7	0.1383	$\times 10^{-13}$	0.1266	$\times 10^{-13}$	0.1239	$\times 10^{-13}$
12	7	-.2264	$\times 10^{-13}$	-.2366	$\times 10^{-13}$	-.2361	$\times 10^{-13}$
13	7	-.3528	$\times 10^{-14}$	-.3696	$\times 10^{-14}$	-.3793	$\times 10^{-14}$
14	7	0.1568	$\times 10^{-14}$	0.1235	$\times 10^{-14}$	0.1238	$\times 10^{-14}$
15	7	0.6315	$\times 10^{-15}$	0.6008	$\times 10^{-15}$	0.5739	$\times 10^{-15}$
16	7	-.6194	$\times 10^{-16}$	-.1235	$\times 10^{-15}$	-.1470	$\times 10^{-15}$
17	7	0.8686	$\times 10^{-16}$	0.8237	$\times 10^{-16}$	0.8542	$\times 10^{-16}$
18	7	0.3222	$\times 10^{-16}$	0.8421	$\times 10^{-17}$	0.4652	$\times 10^{-17}$
19	7	-.6073	$\times 10^{-16}$	-.6665	$\times 10^{-16}$	-.6540	$\times 10^{-16}$
20	7	-.9734	$\times 10^{-16}$	-.7980	$\times 10^{-16}$	-.7171	$\times 10^{-16}$
21	7	-.3029	$\times 10^{-17}$	-.1697	$\times 10^{-16}$	-.1369	$\times 10^{-16}$
22	7	0.3589	$\times 10^{-16}$	0.2181	$\times 10^{-17}$	0.2264	$\times 10^{-17}$
23	7	-.2439	$\times 10^{-16}$	-.1596	$\times 10^{-16}$	-.1466	$\times 10^{-16}$
24	7	-.5551	$\times 10^{-17}$	0.1122	$\times 10^{-16}$	0.1031	$\times 10^{-16}$
25	7	0.8541	$\times 10^{-18}$	-.1011	$\times 10^{-16}$	-.9571	$\times 10^{-17}$
26	7	0.9660	$\times 10^{-17}$	0.8731	$\times 10^{-17}$	0.7996	$\times 10^{-17}$
27	7	-.4681	$\times 10^{-17}$	-.5934	$\times 10^{-17}$	-.5708	$\times 10^{-17}$
28	7	0.6399	$\times 10^{-17}$	0.5632	$\times 10^{-17}$	0.5154	$\times 10^{-17}$
29	7	-.4326	$\times 10^{-17}$	-.3446	$\times 10^{-17}$	-.3351	$\times 10^{-17}$
30	7	0.2032	$\times 10^{-17}$	0.3461	$\times 10^{-17}$	0.3167	$\times 10^{-17}$
31	7	-.2580	$\times 10^{-20}$	-.2022	$\times 10^{-17}$	-.1985	$\times 10^{-17}$
32	7	0.1177	$\times 10^{-17}$	0.2108	$\times 10^{-17}$	0.1930	$\times 10^{-17}$
33	7	-.1715	$\times 10^{-17}$	-.1223	$\times 10^{-17}$	-.1212	$\times 10^{-17}$
34	7	0.1039	$\times 10^{-17}$	0.1308	$\times 10^{-17}$	0.1199	$\times 10^{-17}$
35	7	-.5570	$\times 10^{-18}$	-.9085	$\times 10^{-18}$	-.9098	$\times 10^{-18}$
36	7	0.2491	$\times 10^{-18}$	0.9876	$\times 10^{-18}$	0.9066	$\times 10^{-18}$

TABLE V.2 LEADING PARTITIONS OF THE OBSERVATION MATRIX

EVEN POLYNOMIALS OF ORDER 0:

	0	2	4	6	8	10	
0	1.000	0.349	0.223	0.169	0.139	0.120	0.188 J_0
2	0.349	1.000	0.444	0.310	0.246	0.208	0.052 $\left(\frac{R}{r}\right)^2 J_2$
4	0.223	0.444	1.000	0.480	0.345	0.278	0.026 $\left(\frac{R}{r}\right)^4 J_4$
6	0.169	0.310	0.480	1.000	0.506	0.370	0.016 $\left(\frac{R}{r}\right)^6 J_6$
8	0.139	0.246	0.345	0.506	1.000	0.525	0.011 $\left(\frac{R}{r}\right)^8 J_8$
10	0.120	0.208	0.278	0.370	0.525	1.000	0.008 $\left(\frac{R}{r}\right)^{10} J_{10}$

ODD POLYNOMIALS OF ORDER 0:

	1	3	5	7	9	11	
1	1.000	0.414	0.281	0.220	0.185	0.161	0.089 $\left(\frac{R}{r}\right)^1 J_1$
3	0.414	1.000	0.464	0.329	0.264	0.225	0.035 $\left(\frac{R}{r}\right)^3 J_3$
5	0.281	0.464	1.000	0.494	0.358	0.290	0.020 $\left(\frac{R}{r}\right)^5 J_5$
7	0.220	0.329	0.494	1.000	0.516	0.380	0.013 $\left(\frac{R}{r}\right)^7 J_7$
9	0.185	0.264	0.358	0.516	1.000	0.548	0.009 $\left(\frac{R}{r}\right)^9 J_9$
11	0.161	0.225	0.290	0.380	0.548	1.000	0.007 $\left(\frac{R}{r}\right)^{11} J_{11}$

each row and column is divided by the square root of its diagonal. This is one advantage of using a linearization procedure based on a reference field (IV.6). A procedure based on equation IV.5 would be slightly altitude-dependent even after normalizing the matrix.

On the basis of the small amount of calculation that has been done, it appears the algorithm works. Most of the questions that should arise have to do with the effects of error sources discussed in Section II.4 and the cost of an analysis of this type. Thus, these questions will be examined next.

V.2 Cost of Gradiometer Data Reduction

The cost of a program of this type is of interest. Using the procedure described in Section III.2 the cost of calculating gradiometer readings at a point in space increases as the maximum harmonic degree considered squared since the cost of each harmonic coefficient is a constant and the number of harmonic coefficients increases as the square of the degree. At the same time, the number of points in space that must be considered in a simulation also increases as the square of the degree since there must be more data points than variables. This means the cost of simulating data increases as the fourth power of the maximum harmonic degree being considered. The program used in this study took about seven minutes and would cost about \$85 to perform these operations during prime computer time for 5⁰ blocks.

On the other hand, the cost of reducing gradiometer data on a sphere to harmonic coefficients using the procedure outlined is

composed of two parts: the cost of the theoretical calculations and the inverse, and the cost of expanding the integrals from equation IV.16. The theoretical calculations and inverse only have to be done once and are a small expense in the over-all analysis.

The result of the theoretical calculations is a table of Fourier coefficients for GW_{nm} . This is used to calculate the integrals from equation IV.16 involving the real data. The program involves two steps for these calculations. First the data is integrated with respect to longitude at constant latitude. Then these results are integrated with respect to latitude to obtain coefficients. The time to perform the integration in each step increases as the maximum harmonic degree considered cubed. The program took about one minute and would cost about \$18 to perform these operations during prime computer time for 5⁰ blocks.

The cost of a complete simulation or actual flight data reduction also includes a trajectory analysis. Most of the work for this analysis is common to the simulation part of the analysis performed and it will also increase in cost as the maximum harmonic degree considered to the fourth power. For the entire algorithm a full simulation through harmonic degree 120 (200 to 300 km altitude) would run approximately 60 hours. The trajectory analysis would increase the run time of the simulation part of the algorithm by a constant multiple (like 3) and is required for actual flight data reduction as well as a full scale simulation.

To put this estimate in the proper perspective, the author believes a least squares data reduction technique would increase in

cost as the sixth power of the maximum harmonic degree considered and would take years of computer time at harmonic degree 120. Computer storage is not an especially serious problem for these calculations since the program can be set up to compute one harmonic order at a time in an efficient way. Fitting all the harmonic coefficients into core at one time for the simulation part of the algorithm seems to be the most serious problem one encounters.

V.3 Drifts in the Proportionality Constant

The effect of a drift in the proportionality constant would be precisely the same as a proportional signal if only one complete data set were available. Several procedures can be used to lessen the influence of this type of error. One should estimate the temperature correlation of the scale factor. The instrument manufacturer will supply an estimate of the effect of temperature on the scale factor and this should be used along with satellite engineering data about local temperatures to remove any predictable correlation with temperature.

A more comprehensive procedure would be to consider the data in the vicinity of each of the satellite tracking stations. By assuming a Taylor series expansion for the gravitational field over the station and fitting the coefficients of this field using a least squares technique based on the relatively accurate position data in the vicinity of the tracking station and the gradiometer readings, it should be possible to estimate the scale factor for each pass over each tracing station from the residuals of the least squares fit. Since the satellite must pass over a station at least once every two orbits in

order to unload stored gradiometer readings, this procedure will insure that scale factor variations of the order of the gradiometer sensitivity occurring over a period of one or two orbits can be removed. Generally the satellite passes over a station more often than this so the problem will only be this severe in very remote regions.

Finally, once a field was calculated which would insure the requisite accuracy in the trajectory calculation, it should be possible to use the same local modeling technique to cross couple the data at the north pole and south pole. Since the requirements of the trajectory part of the algorithm are considerably less severe than the potential information available in the data such a procedure should improve the data. In this way the data can be corrected for variations of less than a period of half an orbit ("less than" because the tracking station data is still available). If the trajectory residuals are larger than the instrument sensitivity there is probably no advantage in doing this.

To conclude, the data must be corrected for drifts in the proportionality constant. However, it does not appear difficult to remove errors as large as the instrument sensitivity occurring in a period no shorter than half the period of rotation of the satellite about the earth. Further, the satellite mission can be optimized to help eliminate these errors through the selection of a terminator orbit. A terminator orbit will not go through day/night changes which would cause variations more rapid than this.

V.4 Satellite Orientation Errors

In the preceding section it was assumed that the satellite always pointed in such a way that the earth's radial and the earth's spin axis were in the plane of rotation of the gradiometer. If this is not so, the signal equation will need to be modified since it incorporated this assumption. As long as the true orientation can be measured to sufficient accuracy and the errors are small, there will be no problem in removing this influence from the data.

Again, a reference field formulation is possible. If one assumes one can predict the second derivatives to an accuracy like 1 EU and if one has experimental deviations from the desired trajectory to about 0.1° , a correction can be calculated by operating on the second derivative tensor with the Euler angle transformation composed of the angular errors and identifying the resulting change in signal as the correction. It is necessary to use a full reference field instead of just the mean signal and J_2 term since orientation errors in the region of the equator would not be correctly adjusted otherwise.

In references 10 and 17 it is argued that the procedure will work if the orientation errors are smaller than 0.1° . Since the nutation and precession angles must be controlled to accuracies like 0.1° for precession and 0.001° for nutation (using a passive nutation damper) to overcome dynamics problems, the corrections required are extremely small. All three Euler angles will be available to better than 0.1° accuracies, thus there is no problem making this correction.

V.5 Orbit Determination Errors

Errors in the initial pass through the trajectory determination block are probably the most severe problem with the integral technique just advanced. Clearly if the estimated field data contains large errors due to inaccurate modeling of the gravitational field, the procedure will not converge. In other words, if one computes a correction to a spherical surface based on an inaccurate field, this will introduce errors. In order to assess this problem, the author has resorted to simulation.

What was done was to make use of the gravitational field model referenced earlier to determine how large an error was created by moving data over a variable distance using a truncated version of the same field. The parameters are the distance the data is moved, the harmonic degree at which the field is truncated, and the size of the error. The data was moved radially as this was judged to be most severe. Data points were calculated at the nominal altitude of 830 km and at increments above that using the full field and using truncated fields. The nominal data at each incremental altitude was adjusted to the 830 km altitude by using the difference in the truncated field estimates. The resulting errors are shown in Figure V.2. The location selected for these calculations was over the Indian Ocean low where the total perturbation was nearly 0.4 EU at 830 km. The results indicated that adjustment of the data in this way is not likely to cause problems.

Another type of orbit determination error is possible. If the determination of the position originally is in error, this will result

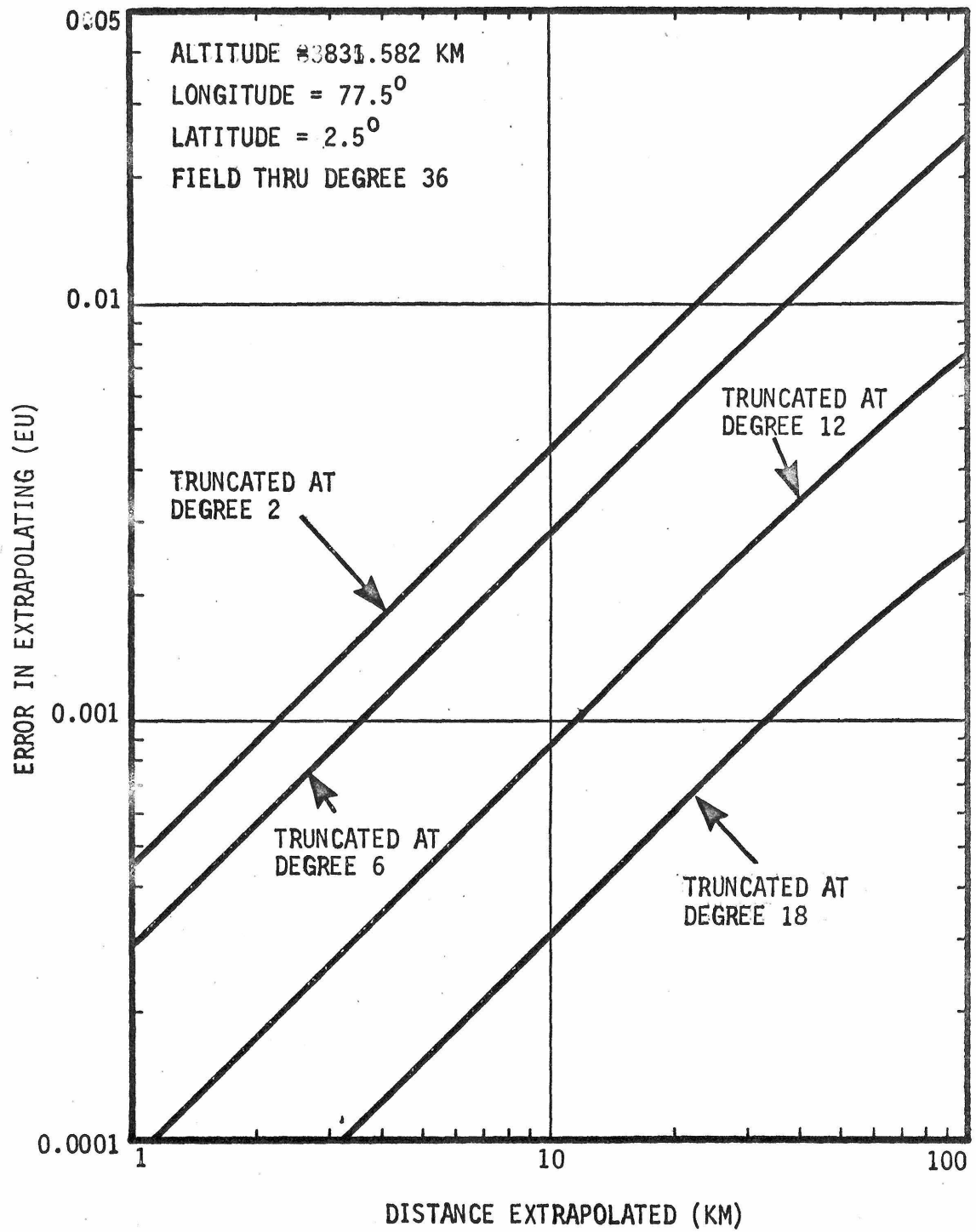


FIGURE V.2 DISTANCE CORRELATED ERRORS IN EXTRAPOLATION TO A SPHERICAL SURFACE

in an error in moving the data of a precisely equivalent amount. The mean signal dominates this error so it is all that needs to be considered. In reference 17 this error has been discussed at some length so the discussion need not be repeated here. The general conclusion is that this type of error is not a problem at the altitudes the gradiometer will fly at if orbit determination could be initially to about 5 meters radially and the instrument sensitivity were 0.01 EU. There is a more stringent requirement than is necessary since the iterative procedure outline will tend to eliminate these errors.

V.6 Spin Rate Effects

Spin rate effects come in two forms: the finite spin rate errors already developed in Section II and the effect of an error in the satellite spin rate, i. e., if the magnitude of the satellite spin rate changed slightly so that it is not equal to the gradiometer resonance frequency. Neither of these problems is especially pervasive unless the gradiometer operates on a resonance principle. Using the data reduction technique proposed, one is in excellent shape to calculate the effect of spin rate errors of either type. One can simply substitute the central force system time variation in place of the latitude and longitude to obtain approximate time histories of the measurement by harmonic coefficient broken down into frequencies. This information can be passed through a transfer function like equation II.5 and the magnitude of the error calculated. This can be done without ever substituting the values of the harmonic coefficients.

The result of this calculation would be a time history of the error which partially depended on experimental data (the time history of the spin rate). This could be applied as a correction at each successive pass of the iteration. It would be possible to correct the bandwidth errors directly by computing an attenuation factor for each coefficient in this way. If this were done, the effect could be incorporated in the basic algorithm. The effect of an error in spin rate could not be treated in this way since it is time variant and consequently could not be integrated over the reference sphere without introducing large errors.

An alternative procedure would be to expand the signal in a Fourier series in time and pass this series through the transfer function from equation II. 5. The resulting series could then be used to calculate corrected data just as if it were real signal. This procedure is undesirable since it would take considerable amounts of computer time and would create errors if the data were not redigitized at a large number more points than the original input data. On the other hand, the calculation would be independent of the spherical harmonic coefficients and thus would not change as the coefficients were improved by the routine.

Finally, if the effect is small enough there is the possibility of developing an empirical formula (x Hz of spin rate error is equivalent to $f(x)$ EU of signal). Such a procedure is not mathematically justified since spin rate errors affect different frequencies in different ways. A more plausible relationship would be of the form x Hz of

spin rate error is equivalent to $f(x)$ EU change in signal from the previous data point. At least this puts the correction on the more rapidly varying part of the field where it belongs.

V.7 The Signal to Noise Ratio

The signal to noise ratio can only be improved through sensor design and by taking more data. If several data sets were available, their average should significantly improve the error calculated from the signal to noise ratio since this error source is truly random.

VI. AN ALGORITHM FOR GRAVITY GRADIOMETER DATA REDUCTION

A brief description of a complete gravity gradiometer data reduction program will be presented.

The algorithm that is about to be advanced has not been entirely programmed. Thus it should be viewed as a proposal rather than a final product. The intent is to clarify the mechanics of a gravity gradiometer data reduction program including the necessary corrections that must be made in conjunction with the iterative calculation of coefficients.

VI. 1 Input Data

The inputs to a gravity gradiometer data reduction program would be as follows: trajectory data, spacecraft engineering data, science data, and the gradiometer data itself. The output of a gravity gradiometer data reduction program would be coefficients of the spherical harmonic expansion of the earth's gravitational field. The input data will be broken down in the following paragraphs.

Trajectory data will be available from the satellite tracking net observing the satellite. It will include time of acquisition and angular position at acquisition for each observation of the spacecraft by each tracking station. The trajectory data may also include range and angular position at regularly spaced time intervals throughout the period of observation of the spacecraft by the tracking station.

The spacecraft engineering data will be transmitted by the spacecraft itself and recorded at the tracking stations. It will include

orientation information relative to the horizon and the sun, spin rate, and temperature data useful for estimating the gradiometer scale factor. Spacecraft engineering data may also include measurement of the in-plane (relative to the spin axis) drag components acting on the spacecraft. A variety of other data will be available of no particular interest to the data reduction system.

The science data includes all the ground truth necessary to do gravity gradiometer data reduction. This includes an initial estimate of the coefficients of the spherical harmonic expansion of the earth's gravitational field, station locations for the satellite tracking net, and a variety of estimates of the amplitudes of perturbations acting on the satellite trajectory. These last considerations include the effects of the sun and moon (which contribute negligibly small gradients), estimates of the atmospheric drag acting on the spacecraft, the effects of wobbles in the earth's spin vector, relativistic effects, etc. This data set is the one which the satellite experiment is intended to improve.

The gravity gradiometer data will consist of amplitude measurements at regularly spaced time intervals from a low circular polar orbit with the satellite spin vector maintained perpendicular to the plane of the orbit and the orbital altitude selected to give repeating ground tracks. A variety of errors will be present in the data as have already been described.

These four types of data will be processed to obtain an improved estimate of the coefficients of the spherical harmonic expansion of the earth's gravitational field. This involves three principle steps. First, the trajectory of the satellite needs to be estimated. Second, the

gradiometer data needs to be adjusted for non-ideal effects. And third, the data needs to be integrated over a sphere to obtain harmonic coefficients. Thus, the data reduction system will follow the flow diagram shown in Figure VI. 1.

VI. 2 The Trajectory Calculation

One is in unusually good shape for calculating a trajectory with the gradiometer. The gradiometer reading is a point function in space, thus the data itself is potentially useful in the trajectory calculation as a check on the initial conditions used. Most orbit determination calculations are done using numerical integration of the equations of motion. The gravitational accelerations are estimated and often the derivatives of the accelerations (gradients) are calculated. Thus all the necessary information to estimate the signal amplitude from a gravity gradiometer is available in a normal numerical integration orbit determination routine.

With a routine of this type it should be relatively easy to compare the measured gradiometer signal amplitude to the signal computed by the routine. A procedure might be developed for minimizing the difference between the two estimates. Further, at least in the case of the Bell Aerospace gradiometer there would be measured drag data available along the flight path. In this way it should be possible to improve on present day trajectory calculations, though it is not essential that any improvement at all be made.

In any event, the trajectory routine would output a satellite ephemeris and also would output estimates for the second derivatives

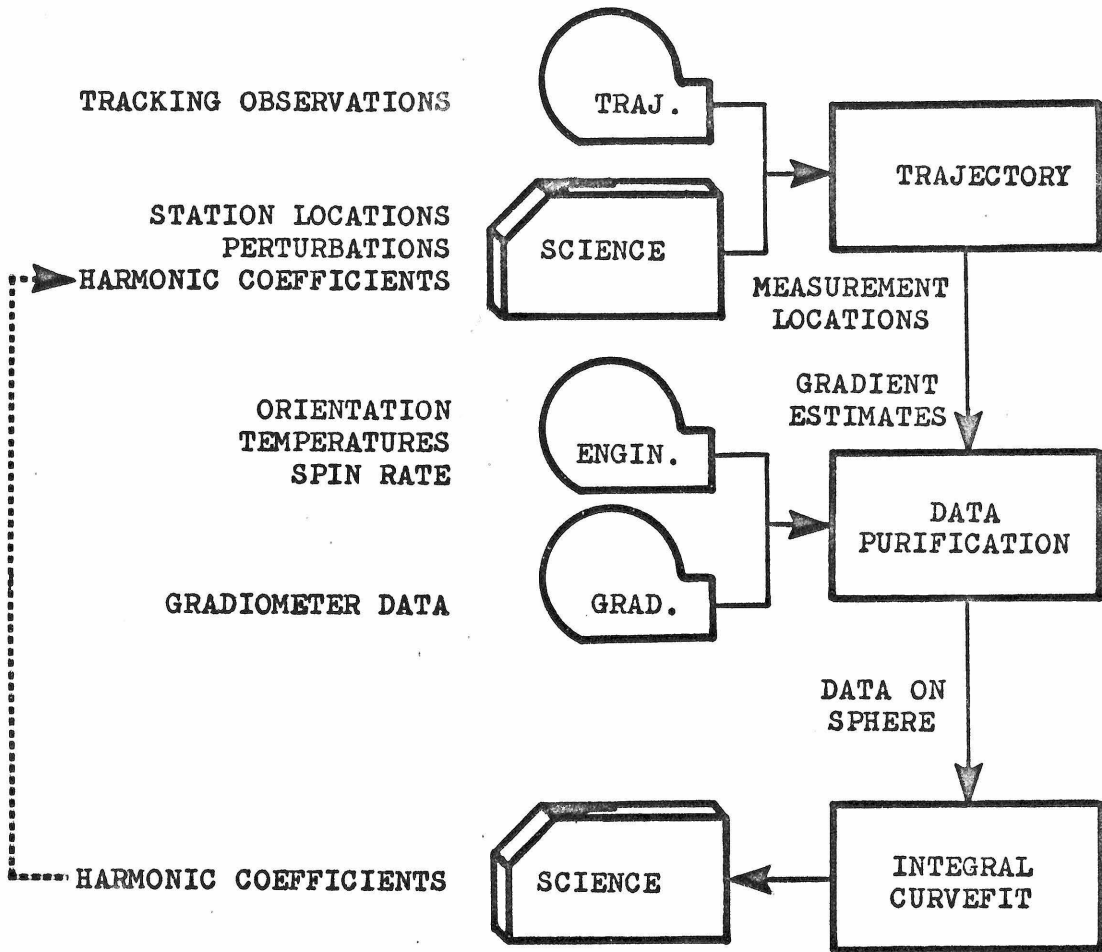


FIGURE VI.1 INTEGRAL CURVEFIT FLOW DIAGRAM

at the location of the satellite computed from the reference field. Since the gradiometer will be reporting an amplitude more often than a trajectory routine would be likely to be set to step, a unit time step could be used equal to the time between gradiometer readings.

VI.3 Data Purification

This step would involve the correction to a spherical surface and adjustment of the individual error sources. The operations in this step are basically filter processes that are either done once or updated at each step in the iteration. The procedures one might use for removing these errors have been described in Section V so they will only be summarized here. The steps to be taken are as follows:

Common filter processes: (only done once)

1. Correct spin rate errors using spacecraft engineering data and equation II.5 with data supplied by the instrument manufacturer (Section V.6).
2. Remove temperature correlated scale factor variations using spacecraft engineering data and a temperature correction supplied by the instrument manufacturer (Section V.3).
3. Remove dynamic errors using spacecraft engineering data.

Updating filter processes: (repeated at each iteration step)

1. Remove orientation errors using spacecraft engineering data and second derivatives estimated by the trajectory routine (Section V.4).

2. Remove scale factor drifts over the tracking stations using gradiometer data and tracking station data (Section V. 3).
3. If the tracking station residuals are small enough to warrant such a procedure, use data from the trajectory routine and gradiometer data to remove scale factor drifts over the poles in conjunction with the step above (Section V. 2).

At this stage the nonlinearity correction and the correction of the data to a spherical surface is left. The signal could be linearized by equation IV. 6, but these operations can be combined using the equation shown below:

$$V_{zz} - V_{xx} \Big|_{b. c.} = \text{Ampl} \Big|_{\text{orbit}}^{\text{meas.}} - (\text{Ampl} \Big|_{\text{orbit}}^{\text{ref.}} - V_{zz} - V_{xx} \Big|_{b. c.}^{\text{ref.}}) \quad (\text{VI. 1})$$

Where b. c. stands for block center, ref. stands for the reference field from the trajectory routine, meas. stands for measured gradiometer data, and so on. One simply computes which block is nearest to the measured point and checks to see if there is data estimated at the block already. If so, one either averages or discards the measured data extrapolated the furthest. Finally, one stores the extrapolated data and proceeds to the next point.

Moving the data in horizontal directions will seem erroneous to Geodacists. At the satellite altitude, if the block size has been selected small enough (roughly equal to the altitude of the satellite),

this is a legitimate approximation since the field has converged and all readings in the same block are very nearly the same. On the surface this is impossible since the corresponding block size is too small for practical calculations.

Before leaving the subject of corrections, a word is in order on the size of correction being applied. Reference 17 defines a set of satellite design constraints which would eliminate orientation corrections entirely, though this appears to complicate the satellite design unnecessarily. Further, depending on the adequacy of the sensor, the temperature corrections may be very small or negligible. Scale factor drifts and mapping the data on a sphere are essential to deal with. Spin rate errors and bandwidth problems are primarily limited to the Hughes sensor. For the Hughes sensor they are extremely serious and must be a factor in the sensor design.

VI.4 Integral Curvefit Calculations

The integral curvefit part of the calculation is probably the most rapid of the elements. One simply fits a two dimensional fast Fourier transform of the spherical data and integrates equation IV.16 with predetermined functions GW_{nm} . The result is a new set of coefficients which can be used in the trajectory calculations.

Calculation of GW_{nm} as a Fourier series is only done once. The procedure was outlined in detail in Section IV so it will only be summarized here. The steps to be taken are as follows:

1. Compute the Fourier expansion of the associated Legendre polynomials for the coefficients of order m (Table IV.2).
2. Compute gradiometer polynomial Fourier expansions of order m (IV.14).
3. Normalize the gradiometer polynomials by the square root of the diagonal of the observation matrix (Figure V.2).
4. Form the observation matrix (IV.10).
5. Invert the observation matrix and multiply times the matrix of Fourier coefficients of G_{nm} (IV.15).
6. Scale the resulting GW_{nm} array so that the coefficients are the variable being dealt with (Figure V.2).

If a narrow bandwidth sensor is being used, step four must be modified to include the attenuation factor of the high frequency part of the harmonic that falls on the edge of the band.

VII. CONCLUSIONS

Reduction of gravity gradiometer data to spherical harmonic coefficients is an exciting possibility. Because of the unique "direct" nature of the measurement, gradiometer data is susceptible to the same types of data reduction techniques as ground based measurements, i. e., integral and least squares curvefit techniques. Because of the possibility of carrying the gradiometer in a satellite, satellite gradiometer data is not susceptible to many of the usual problems of ground based measurement, i. e., poor convergence of the spherical harmonic expansion, the influence of the local terrain, and a lack of global data.

Due to the relatively unworked state of gravity gradiometer data reduction, this thesis has concentrated on the more basic aspects of the problem and in particular representation of the signal in terms of the spherical harmonic expansion. It has been shown that a set of "gradiometer polynomials" can be defined which allow representation of the signal in the same form as the spherical harmonic expansion. Two procedures have been advanced for calculating these polynomials; one based on Legendre polynomials and the other based on Fourier series.

Following classical theory a procedure has been developed for orthogonalizing a truncated system of these polynomials with respect to a set of weighting functions, thus in principle solving the problem of gravity gradiometer data reduction. The practical details of the solution have been programmed. In programming the simulation part of the algorithm, gradiometer polynomials were calculated using the Legendre polynomial approach, while in programming the data

reduction procedure gradiometer polynomials were calculated using the Fourier series approach. The mathematical integrity of the solution has been demonstrated in this way.

This work was closely associated with a satellite feasibility study undertaken by the Jet Propulsion Laboratory (17). The author worked on the JPL study team and has used the same configuration for this study. The work of the two studies are intended to complement each other with the JPL study concentrating on hardware considerations and this study concentrating on software problems. Overall the results of both studies are positive. From the work done to date it appears that a gravity gradiometer satellite can be constructed and a mission defined so that spherical harmonic coefficients can be calculated complete to the order of magnitude of the wave length associated with the satellite altitude.

All this does not mean that a satellite is likely to fly in the immediate future or even that it should fly in the immediate future. A number of areas require further work. In the area of gradiometer data reduction the next logical step would be a complete simulation including the effects of the error sources discussed in Section V and introduced in Section II. The most serious error source is probably introduced by the initial determination of the satellite trajectory. Because of time and cost limitations this error has not been simulated; however, the prospects seem excellent for overcoming this problem.

Orbit responses are completely analogous to the problem of needing a geoid to calculate a geoid. The variations in the trajectory of the satellite can not be as great a problem at satellite altitudes as

the variations in the geoid height is at sea level. The satellite trajectory is smoother than the equipotential surface at the satellite's altitude, which in turn is smoother than the geoid. The correction will introduce smaller errors than the usual free air reduction done on surface data to adjust the data to the geoid. The reason surface acceleration data converges when moved to the geoid is because the acceleration measurement measures a higher derivative than is required to calculate the correction. Thus the measurement is more susceptible to short wave lengths than the correction. A gradiometer measures yet a higher derivative than acceleration. Again the situation is more promising than a procedure which works.

Because of the high cost of a full scale simulation the author does not believe it should be attempted next. A properly scaled simulation at a higher altitude could be made to give just as much information at a considerably lower cost. Other areas are more likely to rule out a gradiometer satellite mission than data reduction. In particular, software needs to be demonstrated to achieve the overall objectives of the earth physics program of which a gradiometer satellite would be a small part. While the objectives of the program as set forward by the National Aeronautics and Space Administration (and briefly discussed in the introduction) are exciting, a more concrete demonstration of what can be achieved should be undertaken in the very near future. It is not at all clear what role gravity data would play in such a program.

REFERENCES

1. "The Terrestrial Environment: Solid-Earth and Ocean Physics" (Williamstown Report). NASA Contractor Report CR-1579, prepared by MIT, Cambridge, Mass., (April 1970).
2. Document not released at time of publication. To be released by office of B. Milwitzky, NASA Headquarters, Washington, D.C. See: "Earth and Ocean Physics Application Planning Study", Document 760-72, prepared by JPL, Pasadena, Ca., (May 1972).
3. Heiskanen, W. and Moritz, H., Physical Geodesy, W. H. Freeman and Company, San Francisco, Ca. (1967).
4. Comfort, G. C., "The Determination of Gravitational Potential from the Measurement of Relative Velocity Between Satellites", Doctoral Thesis at MIT Aerospace Department, Cambridge, Mass., (June 1971).
5. Schwartz, C. R., "Gravity Field Refinement by Satellite to Satellite Doppler Tracking", Reports of the Department of Geodetic Science Report No. 147, Ohio State University, Columbus, Ohio, (Dec. 1970).
6. Rapp, R. H., "Accuracy of Potential Coefficients Determinations from Satellite Altimetry and Terrestrial Gravity", Reports of the Department of Geodetic Science Report No. 166, Ohio State University, Columbus, Ohio, (Dec. 1971).

7. Szabo, B., "Measurement of Gravitational Gradients from Moving Platforms", paper presented at International Symposium on Earth Gravity Models and Related Problems, St. Louis, (Aug. 1972), copy on microfilm from AGU, 1707 L. St., N.W., Washington, D. C.
8. Mueller, I. I., "The Horizontal Gradients of Gravity in Geodesy", Reports of the Department of Geodetic Science, 164 W. 19th Ave., Ohio State University, Columbus, Ohio, (1964).
9. Glaser, R. J. and Sherry, E. J., "Comparison of Satellite Gravitational Techniques", paper presented at International Symposium on Earth Gravity Models and Related Problems, St. Louis, (Aug. 1972), copy on microfilm from AGU, 1707 L St., N.W., Washington, D. C.
10. Hughes Research Laboratory, Part 2, Technical Proposal No. 71 M-1173/C4163, "Lunar Orbiting Gravity Gradiometer Development", Malibu, Ca., (March 1971).
11. Bell Aerospace Company, Proposal No. D6324-953001, "Proposal for a Prototype Moving-Base Gravity Gradiometer", Buffalo, New York, (March 1971).
12. DeBra, D., Internal report on gradiometer dynamics contracted by JPL, expanded and published in reference 13 below, Stanford University, Palo Alto, Ca.
13. Peterson, R. W., "Dynamic Analysis of the Second Order Gradiometer", Hughes Research Laboratory Report 441, Hughes Research Laboratory, Malibu, Ca., (July 1971).

14. Mallove, E. F., "An Improved Dynamic Analysis of the Second Order Gradiometer", Hughes Research Laboratory Report 451, Hughes Research Laboratory, Malibu, Ca., (Feb. 1972).
15. Whittaker, E. T. and Watson, G. N., A Course of Modern Analysis, The University Press, New York (1902), reprinted 1947.
16. Goldstein, H., Classical Mechanics, Addison-Wesley Press, Inc., Cambridge, Mass (1950).
17. Jet Propulsion Laboratory, Document No. 760-70, "Earth Physics Satellite Gravity Gradiometer Study", JPL, Pasadena, Ca., (May 1972).
18. Hopkins, J., "Unclassified Earth Gravity Model", unpublished, ACIC, St. Louis, Missouri.